



HAL
open science

Chloeia rozbaczyloi, a new species of polychaete (Archinominae: Amphinomidae) and first record of the family for the Nazca Ridge, southeastern Pacific Ocean

Juan I Cañete, María S Romero, Erin E Easton, Ariadna Mecho, Javier Sellanes

► To cite this version:

Juan I Cañete, María S Romero, Erin E Easton, Ariadna Mecho, Javier Sellanes. *Chloeia rozbaczyloi*, a new species of polychaete (Archinominae: Amphinomidae) and first record of the family for the Nazca Ridge, southeastern Pacific Ocean. *Deep Sea Research Part I: Oceanographic Research Papers*, In press, pp.104110. 10.1016/j.dsr.2023.104110 . hal-04164864

HAL Id: hal-04164864

<https://hal.science/hal-04164864v1>

Submitted on 18 Jul 2023

HAL is a multi-disciplinary open access archive for the deposit and dissemination of scientific research documents, whether they are published or not. The documents may come from teaching and research institutions in France or abroad, or from public or private research centers.

L'archive ouverte pluridisciplinaire **HAL**, est destinée au dépôt et à la diffusion de documents scientifiques de niveau recherche, publiés ou non, émanant des établissements d'enseignement et de recherche français ou étrangers, des laboratoires publics ou privés.

Journal Pre-proof



Chloeia rozbaczyloi, a new species of polychaete (Archinominae: Amphinomidae) and first record of the family for the Nazca Ridge, southeastern Pacific Ocean

Juan I. Cañete, María S. Romero, Erin E. Easton, Ariadna Mecho, Javier Sellanes

PII: S0967-0637(23)00149-8

DOI: <https://doi.org/10.1016/j.dsr.2023.104110>

Reference: DSRI 104110

To appear in: *Deep-Sea Research Part I*

Received Date: 5 September 2022

Revised Date: 10 July 2023

Accepted Date: 13 July 2023

Please cite this article as: Cañete, J.I., Romero, Marí.S., Easton, E.E., Mecho, A., Sellanes, J., *Chloeia rozbaczyloi*, a new species of polychaete (Archinominae: Amphinomidae) and first record of the family for the Nazca Ridge, southeastern Pacific Ocean, *Deep-Sea Research Part I* (2023), doi: <https://doi.org/10.1016/j.dsr.2023.104110>.

This is a PDF file of an article that has undergone enhancements after acceptance, such as the addition of a cover page and metadata, and formatting for readability, but it is not yet the definitive version of record. This version will undergo additional copyediting, typesetting and review before it is published in its final form, but we are providing this version to give early visibility of the article. Please note that, during the production process, errors may be discovered which could affect the content, and all legal disclaimers that apply to the journal pertain.

© 2023 Published by Elsevier Ltd.

1 ***Chloeia rozbaczyloi*, a new species of polychaete (Archinominae: Amphinomidae)**
2 **and first record of the family for the Nazca Ridge, southeastern Pacific Ocean**

3
4 Juan I. Cañete¹, María S. Romero², Erin E. Easton^{3,4}, Ariadna Mecho^{4,5} and Javier
5 Sellanes^{4,6*}
6

7 1.- Departamento de Ciencias y Recursos Naturales, Facultad de Ciencias, Universidad
8 de Magallanes, Punta Arenas, Chile.

9 2.- Laboratorio Microscopia Electrónica, Facultad de Ciencias del Mar, Universidad
10 Católica del Norte, Coquimbo, Chile.

11 3.- School of Environmental, Earth, and Marine Sciences, University of Texas Rio
12 Grande Valley, Brownsville, TX.

13 4.- Center for Ecology and Sustainable Management of Oceanic Islands (ESMOI),
14 Universidad Católica del Norte, Coquimbo, Chile.

15 5.- Laboratoire des Sciences du Climat et de l'Environnement (LSCE/IPSL), CEA/Saclay,
16 Gif-sur-Yvette, France

17 6.- Departamento de Biología Marina, Facultad de Ciencias del Mar, Universidad
18 Católica del Norte, Coquimbo, Chile.

19
20 * Corresponding author: sellanes@ucn.cl; Tel: +56 962203515

21 **Abstract (327 words)**

22 The amphinomid polychaete *Chloeia rozbaczyloi* sp. nov., collected from seamounts of
23 the Nazca Ridge (NR), northwest of Desventuradas islands, southeastern Pacific Ocean,
24 is described. The new species was observed on only two of seven seamounts surveyed in
25 the area (25.079°S, 82.006°W, and 25.408°S, 81.769°W, ~220 m depth), being abundant
26 on one of them.

27 Specimens were observed under optical and scanning electron microscopes, and
28 DNA was sequenced (COI, 16S, 18S, and 28S nucleotide alignment). *Chloeia rozbaczyloi*
29 sp. nov. belongs to the *venusta* group of *Chloeia* and is distinguished mainly by: (i) the
30 chromatic pattern of the dorsum (with a single middorsal dark band) and the caruncle
31 (with 16 to 20 vertical folds and 12 to 14 black spots posteriorly decreasing in diameter),
32 (ii) by the bi-annulated dorsum of the first ten chaetigers, each with a bean-shaped anterior
33 pseudosegment, (iii) long neuropodial cirri, with a short ceratophore, at chaetiger 2 and
34 reaching chaetiger 6, and (iv) bipinnate branchiae from chaetiger 4, with seven to nine
35 lateral branches arising from the primary axis, each passing five pinnules; branchiae
36 change progressively in size to the posterior end. The ciliated margin of the accessory
37 dorsal cirri suggests a respiratory function that might be relevant considering that both
38 seamounts in which the species was observed could be influenced by low-oxygen waters.
39 DNA results further support that *C. rozbaczyloi* sp. nov. differs from the other five
40 congeneric taxa (*C. bimaculata*, *C. flava*, *C. parva*, *C. pocicola*, and *C. viridis*) for which
41 genetic information is available.

42 This finding constitutes the first report of the genus for Chilean waters, increasing
43 the number of species of Amphinomidae in this area to seven. It also confirms the
44 presence of the family in the NR and increases the number of *Chloeia* species in the world
45 to 43.

46 The seamounts where the new species have been collected are within the newly
47 created offshore Nazca-Desventuradas Marine Park. Information on potentially unique
48 and endemic species, such as the one discussed here, is of utmost importance to preserve
49 special ecological units, address ecosystem services, and implement management
50 measures in the area.

51

52 Keywords: fireworm; deep sea; seamount; Nazca-Desventuradas Marine Park; Chile,
53 Archinomidae.

54 This article is registered in ZooBank under urn:lsid: zoobank.org:pub:3F142A93-1679-
55 4192-AA75-8B71CA0A79F4

56 **Introduction**

57 *Chloeia* Lamarck, 1818 is one of the 18 recognized genera of Amphinomidae
58 (Polychaeta), known as fireworms for the burning sensation felt by humans in response
59 to exposure to the setal-associated neurotoxin produced by some species (Kudenov,
60 1995). Although the family is distributed globally in most marine environments
61 (Kudenov, 1995; Rouse and Pleijel, 2001; Böggemann, 2009; Wang et al., 2019; Yáñez-
62 Rivera and Salazar-Vallejo, 2022; Salazar-Vallejo, 2023), *Chloeia* species have a more
63 circumtropical distribution, occurring mostly at shallow depths and being more speciose
64 in the Indian and Pacific than in the Atlantic Ocean (Salazar-Vallejo, 2023). *Chloeia*
65 species are characterized by having an elliptical body, with bipinnate branchiae (Barroso
66 and Paiva, 2011), notopodial cirri, cirrophores, and a caruncle (Kudenov, 1995, Barroso
67 et al., 2021). They have species-specific dorsal pigmentation patterns, which are often
68 violet, green, yellow, black, and reddish brown/black (Kudenov, 1995; Yáñez-Rivera and
69 Salazar-Vallejo, 2022). Other taxonomically informative characters include relative size
70 and development of the caruncle; length of second parapodial cirri; chaetae number,
71 distribution along body, and shape; types of notochaetae, neurochaetae, and pygidial cirri;
72 distribution, development, and placement of branchiae; degree of development and type
73 of anal cirri as a proportion of sizes of the eyes; and caruncle pigmentation pattern
74 (Kudenov, 1995; Barroso and Paiva, 2011; Wang et al., 2019; Yáñez-Rivera and Salazar-
75 Vallejo, 2022; Salazar-Vallejo, 2023). Polychaetes are known to have significant changes
76 in the size of eyes, shape of parapodia, caruncle pigmentation and chaetae during epitoky
77 period (Rouse & Pleijel, 2001), especially in amphinomids (Salazar-Vallejo, 2023). Most
78 *Chloeia* species have branchiae beginning from the chaetiger 4 (Table 1); species with
79 branchiae beginning from chaetiger 5 have been reported for the southern parts of the
80 Indian and Pacific oceans (Barroso and Paiva, 2011; Barroso et al., 2021; Yáñez-Rivera
81 and Salazar-Vallejo, 2022; Salazar-Vallejo, 2023).

82 Except for a single mention of the genus *Chloeia* for some seamounts of the Salas
83 y Gómez Ridge by Parin et al. (1997), no species of the genus have been reported for
84 other seamounts or ocean ridges worldwide, despite some *Chloeia* occurring in the deep-
85 sea (Barroso and Paiva, 2011). The latter include the recently described *C. pocicola* from
86 pockmark fields off the Brazilian coast at ~750 m depth (Barroso et al., 2021) and *C.*
87 *pinnata*, which shows a wide bathymetric distribution ranging from 20 to 1900 m depth

88 (Jones and Thompson, 1987; Yáñez-Rivera and Salazar-Vallejo, 2022). Of the 42
 89 currently accepted species (Wang et al., 2019; Read and Fauchald, 2023, Barroso et al.
 90 2021; Yáñez-Rivera and Salazar-Vallejo, 2022; Salazar-Vallejo, 2023), nine occur in the
 91 Atlantic Ocean (including the Mediterranean Sea), 12 in the Indian Ocean, 13 in the Indo-
 92 west Pacific, and seven in the eastern or southern Pacific Ocean. Of the species at least
 93 partially distributed in the Pacific Ocean, five have been described from the northwestern
 94 Pacific (*C. bimaculata*, *C. conspicua*, *C. fusca*, *C. incerta*, and *C. pulchella*), seven from
 95 the central and the eastern Pacific (*C. fusca*, *C. murrayae*, *C. nuriae*, *C. pinnata*, *C.*
 96 *poupini*, *C. pseuglochis* and *C. richeri*), and one from the southern Pacific (*C. inermis*)
 97 (Yáñez-Rivera and Salazar-Vallejo, 2022; Salazar-Vallejo, 2023). Before the present
 98 study, only six species of Amphinomidae were reported from Chilean waters (Kudenov,
 99 1993; Rozbaczylo 1985; Cañete 2017); half of them for Rapa Nui (Easter Island) [i.e.,
 100 *Eurythoe complanata* (Pallas, 1776), *Pherecardia striata* (Kingberg, 1857) and
 101 *Linopherus* sp. (Kohn and Lloyd, 1973; Cañete, 2017)]. The other three species,
 102 *Paramphinome australis* Monro, 1930, *Pareurythoe chilensis* (Kingberg, 1857), and
 103 *Linopherus annulata* Hartmann-Schröder, 1965, are respectively distributed between
 104 Arica (northern Chile) and Antarctica (25 to 1180 m depth), between Valparaíso and
 105 Chiloé Island (13 to 260 m depth), and around Mocha Island and Galera Point (26 to 160
 106 m depth) (Rozbaczylo, 1985). No prior reports of the family exist in the literature for the
 107 Nazca Ridge (NR) seamounts and islands, a zone that seems to be prolific in new species
 108 of polychaetes (Díaz-Díaz et al., 2020).

109 In this study, we (i) describe *Chloeia rozbaczyloi* sp. nov, the first species of the
 110 genus reported for seamounts of the NR within Chilean jurisdiction, (ii) provide
 111 preliminary information on its abundance and habitat, and (iii) provide some insight into
 112 the function of the accessory dorsal cirri. In addition, we provide sequence data for the
 113 partial mitochondrial genome and 18S-to-28S rRNA gene fragment and infer the genetic
 114 relationship between *C. rozbaczyloi* sp. nov. and other congeneric species based on
 115 available genetic data.

116

117 Abbreviations

118 CIMAR	Program for Oceanographic Exploration of Remote Jurisdictional Marine
119	Areas, funded by the National Oceanographic Committee of Chile,
120	Chilean Navy.
121 BL	Body length.
122 MNHNCL	Museo Nacional de Historia Natural, Santiago, Chile.

123	NDMP	Nazca-Desventuradas Marine Park.
124	NR	Nazca Ridge.
125	OMZ	Oxygen Minimum Zone.
126	ROV	Remotely Operated Vehicle.
127	SCBUCN	Sala de Colecciones Biológicas, Universidad Católica del Norte, Facultad
128		de Ciencias del Mar, Coquimbo, Chile.
129	SEM	Scanning Electron Microscope
130		

131 **Materials and Methods**

132 During the multidisciplinary oceanographic cruise CIMAR 22 “Oceanic Islands”, carried
133 out onboard RV *Cabo de Hornos* between October and November 2016, the benthic
134 habitat and fauna of unexplored seamounts of the Juan Fernández and Desventuradas
135 Ecoregion (Spalding et al. 2007; ecoregion number 179) were surveyed by remotely
136 operated vehicle (ROV) and from bottom trawling (Tapia-Guerra et al., 2021, Tapia et
137 al., 2021) (Fig. 1). Habitat characterizations and relative abundance of the benthic
138 epifauna were performed from video observations using an ROV (model Commander
139 MKII, Mariscop Meerestechnik, Kiel, Germany) equipped with an HD Camcorder
140 (Panasonic SD 909) and laser pointers (10 cm apart). A total of 11 video transects were
141 performed within the NDMP between 130 and 370 m depth; six transects at NR
142 seamounts and five around the Desventuradas Islands (Fig. 1A). After ROV surveys,
143 samples were collected by 10-min hauls (bottom contact), at ~3 knots, using a modified
144 Agassiz trawl that consisted of a metal frame with a mouth of 2 × 0.5 m (width × height)
145 fitted with a net of 12-mm mesh at the cod end.

146 Individuals of a locally abundant fireworm belonging to the Amphinomidae were
147 observed and collected at seamount SFX (Fig.1 B), one of the seven seamounts surveyed
148 during the cruise (Fig. 1). Collected specimens were preserved in 100% ethanol.
149 Additional specimens were subsequently collected, following the same collection and
150 preservation methods, from ~250 m depth at another seamount (SPG4; Fig. 1) located
151 ~22 nm southeast of the original locality (seamount SFX). This seamount was the only
152 seamount of the NR surveyed during the EPIC (Eastern Pacific International Campaign)
153 cruise (RV *Mirai*). Sample collection was done under the permission Res. Ext
154 N°3685/2016 and N°4508/18 from SUBPESCA (Chile) to Universidad Católica del
155 Norte. All specimens were preserved onboard following the protocols described above
156 and initially deposited at SCBUCN.

157 The following morphological characters were examined: maximum body width
158 (excluding chaetae), body length (prostomium to pygidium), number of chaetigers,
159 length, shape, number of vertical folds, and free posterior zone of the caruncle, size along
160 the body and number of lateral branches and pinnules in each lateral branch, number of
161 accessory dorsal cirrus, size of ventral cirri, chaetal lobes, chaetal shapes and changes
162 along the body, and dorsal chromatic pattern. Cephalic terminology follows Orrhage
163 (1990), Kudenov (1993, 1995), Barroso and Paiva (2011), Borda et al. (2015), and a
164 recent proposal by Yáñez-Rivera & Salazar-Vallejo (2022) and Salazar-Vallejo (2023).
165 The taxonomic description of amphinomid specimens was based on Kudenov (1993),
166 Liñero-Arana and Díaz (2010), Borda et al. (2012, 2015), Wang et al. (2019), Barroso et
167 al. (2021), Yáñez-Rivera and Salazar-Vallejo (2022), and Salazar-Vallejo (2023). The
168 general description was performed under stereoscopic microscopy and is based on a 35-
169 mm-long specimen (Holotype MNHNCL ANN-15017). Additional specimens (paratypes
170 SCBUCN 6981- 6984) were examined and photographed under a Hitachi SU3500
171 scanning electron microscope (SEM) at the Microscopy Laboratory of the Facultad de
172 Ciencias del Mar, Universidad Católica del Norte, Coquimbo, Chile. Specimens
173 examined with SEM were fixed in ethanol, dehydrated through a graded ethanol series,
174 dried in a Tousimis, Samdri-780A critical-point dryer using CO₂, mounted on bronze
175 stubs, and coated with gold in a JEOL JFC-100 evaporator. The type material was
176 deposited in the MNHNCL and SCBUCN, including specimens prepared for SEM
177 analysis. The description is complemented by observations of living specimens in their
178 natural habitat as documented by images taken by ROV (Fig. 2).

179 DNA was extracted from specimen SCBUCN 6857 using a PureLink Genomic
180 DNA Purification Kit (Invitrogen, Waltham, Massachusetts, USA) per manufacturer's
181 protocol, with a 60-min incubation (55°C at 700 rpm) in a Thermomixer (Eppendorf,
182 Hamburg, Germany) and elution with 50 µl of nuclease-free water. Extracted DNA was
183 submitted to Biopolymers Facility at Harvard Medical School for library preparation
184 (Illumina Nextera XT2) and next-generation sequencing (NextSeq 500). The *18S-ITS1-*
185 *5.8S-ITS2-28S* fragment was recovered following Easton and Hicks (2020) by using
186 software installed on the University of New Hampshire Bioinformatics Core facility RON
187 server, which is supported by the New Hampshire-INBRE Program through an
188 Institutional Development Award, P20GM103506, from the National Institute of General
189 Medical Sciences of the NIH and Geneious Prime 22.0.1 (<https://www.geneious.com>).
190 Because the complete mitochondrial genome was not recovered by those methods, reads

191 were iteratively mapped to *C. pocicola* (MT822294) mitochondrion (complete genome),
192 which is the only complete mitochondrial genome for *Chloeia*, and the resulting
193 consensus sequences with Geneious Prime. Details of these methods and more expansive
194 genetic methods are available in the Supplementary Material. The partial mitochondrial
195 genome and the *18S-ITS1-5.8S-ITS2-28S* fragment were annotated with Live Annotate
196 and Predict in Geneious, respectively, with annotations from *C. pocicola* and *Panthalis*
197 *oerstedii* (KY753846). Results from the MITOS Webserver ([http://mitos.bioinf.uni-](http://mitos.bioinf.uni-leipzig.de/index.py)
198 [leipzig.de/index.py](http://mitos.bioinf.uni-leipzig.de/index.py); Bernt et al. 2013) were used to modify the position of the tRNAs.
199 Protein and rRNA gene annotations were manually adjusted based on alignment with *C.*
200 *pocicola* genes and congruency in presence of predicted start and stop codons between
201 the species. The annotated mitogenome and unannotated *18S-ITS1-5.8S-ITS2-28S* were
202 submitted to GenBank (OM144973 and OM135245, respectively). For the mitochondrial
203 genome sequence, percentage identity between *C. pocicola* and *C. rozbaczyloi* sp. nov.
204 nucleotide and amino acid sequences were calculated based on MUSCLE nucleotide and
205 Geneious amino acid alignments as implemented in Geneious Prime with default
206 parameters; stop codons and missing bases and amino acids were excluded from the
207 alignments, which were trimmed to the shortest extent of aligned genes.

208 For phylogenetic reconstruction based on a concatenated alignment of *28S* rRNA,
209 *16S* rRNA, and *COI* gene fragments, we selected one representative from each *Chloeia*,
210 *Archinome*, and *Notopygos* species for which sequences were available for each of the
211 three gene regions; *Paramphinome jeffreysii* was selected as the outgroup for all
212 reconstructions (Supplementary Material Table S1). Although *18S* rRNA gene fragments
213 were publicly available for most representatives, this gene was excluded from the study
214 because some sequences were missing data or were suspect based on large divergences
215 from the other representatives and most remaining representatives had identical
216 haplotypes for congeners, so the *18S* rRNA gene fragment lacked informative characters
217 for species-level assignments. Sequences were aligned with default Muscle parameters as
218 implemented by Geneious Prime and trimmed to their shortest extent. Genetic similarities
219 (uncorrected p) are reported based on the concatenated and single-gene alignments.
220 Following Xia et al. (2003) and Xia and Lemey (2009), the third codon position of the
221 *COI* gene was removed before phylogenetic reconstruction, leaving a 394 bp alignment,
222 because this codon position was saturated ($p = 0.0096$, $I_{ss} = 0.7278$, $I_{ss,c} = 0.6409$) as
223 determined by the Xia et al. (2003) test of substitution saturation in DAMBE7 (Xia 2018)
224 and therefore is not useful in phylogenetic reconstruction. These single-gene alignments

225 were concatenated (28S + 16S + COI) in Geneious Prime into a 1452 bp alignment (735
226 + 323 + 394 bp, respectively), and the best model of nucleotide evolution was selected
227 with PartitionFinder 2.1.1 (Lanfear et al., 2017) with the following settings:
228 branchlengths=unlinked, models = all with --raxml code (Stamatakis, 2014),
229 model_selection = aicc, search = greedy (Lanfear et al., 2012), and data blocks defined to
230 each gene boundary with protein-coding genes split into the two codon positions for a
231 total of four data blocks. The best scheme selected was to retain the four data blocks as
232 separate partitions with GTR+G selected as the model for *COI* codon position 2 and
233 GTR+I+G as the model for the other three partitions. Because RAxML allows only a
234 single model of rate heterogeneity in partitioned analyses and GTRG+I+G was selected
235 for most partitions, the maximum-likelihood (ML; Felsenstein 1981) phylogenetic tree
236 was constructed in RAxML 8.2.11 (Stamatakis 2014) with nucleotide model = GTR
237 GAMMA I, 100 bootstrap replicates (rapid bootstrapping with a search for best-scoring
238 ML tree), and no outgroup. The best models and partitions were used as prior parameters
239 to reconstruct phylogenies with MrBayes 3.2.6 (Huelsenbeck and Ronquist, 2001) as
240 implemented by Geneious Prime with the selected outgroup (*Paramphinome jeffreysi*),
241 10,000,000 generations, sample frequency of 1000, 4 Markov Chain Monte Carlo, a
242 temperature of 0.2, and burnin of 2500. The final trees were obtained with a 50%
243 majority-rule consensus, and bootstrap values from RAxML phylogenetic trees were
244 added to the nodes. Commands for all phylogenetic reconstructions and details of single-
245 gene phylogenetic reconstructions are available in the Supplementary Material.

246 This published work and the nomenclatural acts it contains were registered in
247 ZooBank (LSID urn:lsid:zoobank.org:pub:3F142A93-1679-4192-AA75-
248 8B71CA0A79F4).

249

250 **Results**

251 *Collections and habitat.* At seamount SFX (Fig. 1), 64 specimens were collected on 31
252 Oct 2016 at ~230 m depth. *Chloeia rozbaczyloi* sp. nov. was abundant (Fig. 2A-G),
253 usually patched in small groups with maximums of ~7 specimens per 100 cm². Sea-
254 bottom observations at seamount SFX revealed calcareous sediments produced by
255 foraminiferous tests, debris of deep-sea corals, holopelagic gastropod shells, and
256 rhodoliths (Fig. 2A-D). Other taxa representative of this station were anthozoans

257 (unidentified anemones, Fig. 2A-B), a fasciolarid gastropod (*Chryseofusus kazdailisi*,
258 Fig. 2E), and the irregular echinoid *Scrippsechinus fisheri* (Fig. 2F).

259

260 *Systematics*

261 Family Amphinomidae Lamarck, 1818

262 Subfamily Archinominae Kudenov, 1991

263 Genus *Chloeia* Lamarck, 1818

264 Type species. *Aphrodita flava* Pallas, 1766, accepted as *Chloeia flava* (Pallas, 1766) by
265 subsequent designation.

266 *Chloeia rozbaczyloi* sp. nov. Cañete and Sellanes

267 Figures 2 B-D, F, G; 3 A-F; 4 A-G; 5; 6 A-G; 7; 8; Table 1; Supplementary Material.

268

269 LSID urn: lsid: zoobank.org:act:574C45FA-EBE7-4614-AB33-E5B9E21CA3F3

270 *Material examined.* Eight specimens: Holotype (MNHNCL ANN-15017) and seven
271 paratypes (SCBUCN 6981-6984, 6857, 6859, and 7262) from seamount SFX, 25.079°S,
272 82.006°W, Agassiz trawl, 220-230 m depth, *RV Cabo de Hornos*, CIMAR 22 cruise, 31
273 Oct. 2016. Additional material: 22 specimens (SCBUCN 8529), all from unnamed
274 seamount Sta. SPG4, 25.408°S, 81.769°W, Agassiz trawl, ~211 m depth, *RV Mirai*, EPIC
275 cruise, 2 Feb. 2019.

276

277 *Diagnosis.* Body fusiform, with 30 segments. Anterior ten chaetigers with central dorsum
278 bi-annulated; complete segment dorsally separated by an anterior bean-shaped
279 pseudosegment; dark middorsal band surrounded by white areas. Trilobate caruncle
280 extending to chaetiger 4, fused to dorsum on chaetigers 1 to 2, free thereafter; with
281 median plicate lobe with 16 to 20 vertical folds and 10 to 14 black spots decreasing in
282 size toward the posterior end; first two black spots hourglass shaped. First three chaetigers
283 with an accessory dorsal cirrus; accessory dorsal cirrus without ceratophores and lateral
284 margin of mid-central region ciliated. Bipinnate branchiae from chaetiger 4, progressively
285 smaller towards posterior region; bifurcate harpoon notochaetae without spurs; thin
286 furcate neurochaetae. Neuropodial cirri of second chaetiger long, with short ceratophore,
287 reaching chaetiger 6.

288

289 *Type locality.* Seamount SFX, at ~230 m depth. Initial geographic position: 25.079°S,
290 82.006°W; final position 25.085°S, 82.015°W. 31 Oct. 2016.

291

292 *Description.* Holotype (MNHNCL ANN-15017), complete specimen BL of 35 mm by 9
293 mm wide (excluding chaetae) in the middle of the body, 28 chaetigers. Specimen with
294 body dorsally flattened, depressed, oval, whitish alive, with gills brown to violet in color;
295 caruncle black, with white band in the lateral margin; all cirri, antennae, and palps
296 whitish. Notochaetae transparent while neurochaetae are whitish; neurochaetae longer
297 than notochaetae. Mid-body dorsum slightly darker than anterior and posterior segments
298 (Fig. 2B, C, F, G). Specimens preserved in alcohol white, with the mid-funnel ventral
299 zone slightly dark (3A-B). Paratypes SCBUCN 6981, 6982, 6983, and 6984 incomplete,
300 sectioned for SEM analysis. Paratype SCBUCN 6859 and 7262 used for stereoscopic
301 microscopy of the anterior end.

302 Trilobate caruncle extending to chaetiger 4, tapered, slightly twisted (Fig. 3C, 4A,
303 5A), with median plicate lobe with 16 to 20 vertical folds and with 10 to 14 black spots
304 decreasing in size to posterior end; first two black spots slightly hourglass shaped;
305 caruncle fused to dorsum between chaetigers 1 to 2; free thereafter (Fig. 3C, 4A, 5A).
306 Posterior lobe of the prostomium with two pairs of black eyes hidden under the anterior
307 margin of the base of the caruncle; anterior pair larger than posterior pair (2:1 in size
308 proportion) and externally detectable in most preserved specimens (Fig. 5A).

309 First ten segments dorsally bi-annulated, of which the anterior pseudosegment is
310 smaller (~1:3 in proportion of total segment length) and bean-shaped (Fig. 3D). From
311 chaetiger 11 on, dorsal zone of each segment white, divided by a mid, narrow and
312 elongated, screw-shaped dark mark. This feature is evident in live specimens (Fig. 3F).

313 Median antennae arising from anterior margin of caruncle; palpal antennae arising
314 from anterior margin of prostomium; lateral antennae anteriorly to median antennae;
315 palpal and lateral antennae of similar length and shape; median antennae longer than
316 paired/palpal antennae (Fig. 4A, B). Median antennae extending to the sixth or seventh
317 folded side of the caruncle or to chaetiger 2; style moderated in length, cylindrical, being
318 shorter than caruncle and of similar length and thickness to lateral antennae; all antennae
319 without ceratophores (Fig. 4B). Palps fused, dorsally ending in a heart shape lobe, semi-
320 grooved; palps converging mid-ventrally into longitudinal groove, leading to mouth (Fig.
321 4B). Mouth located between palps and posterior lip formed by incomplete segment of
322 second and third chaetigers; posterior margin of buccal area with 5 to 6 folds

323 anteroposteriorly oriented and projected toward the fourth chaetiger; first two chaetigers
324 of small size, incomplete ventrally and bordering mouth area (Fig. 4C). Ventral cirrus of
325 chaetiger 2 cirriform, longer and wider than the ventral cirrus of the first five chaetigers
326 (4:1 length ratio); ventral cirrus from six to twenty segments long, with styles 5–7 times
327 longer than cirrophore; long ventral cirrus of second chaetiger directed to the dorsal zone
328 and extending to chaetiger 6 (Fig. 4C).

329 Dorsal cirri of first three chaetigers with ciliated accessory cirrus that is one-sixth
330 the length of the dorsal cirrus; accessory cirrus without ceratophore; lateral margin of
331 accessory cirrus with ciliated edges; distal end not ciliated (Fig. 4D-E).

332 Branchiae best developed in mid-chaetigers, decreasing progressively in size to
333 posterior end; branchiae bipinnate from chaetiger 4 to the end of body, in general with
334 seven lateral branches (up to nine in some mid-chaetigers), arising from the primary axis,
335 each having five short pinnules (Fig. 4F, 5B); each branch located in lateral position and
336 well separated from one another; branchiae inserted slightly displaced posterior to the
337 notopodial lobe, close to intersegmental groove (Fig. 4F). Branchiae shorter than dorsal
338 cirrus (1:2) (Fig. 4F).

339 Pygidium terminal, opening between a pair of thick, digitiform anal cirri, with
340 dorsal anus (Fig. 4G). Pygidial cirrus extending to the last five chaetigers. Ventral cirrus
341 of the last chaetiger with short cirrophores, ~10% of the total length of cirrostyle (Fig.
342 4G).

343 Parapodia well developed with widely separated rami in all chaetigers (Fig. 4A,
344 4D). Parapodia biramous, notopodia with short accessory and dorsal cirri and neuropodia
345 with single ventral cirrus. First and second chaetigers with lobes reduced in size and
346 directed dorsally, with fascicles of gross bidentate chaetae facing to the back (Fig. 4A).
347 Neuropodial cirri of second chaetiger long, with short ceratophore, reaching chaetiger 6
348 (Fig. 4C)

349 Notochaetae change along the body, of four types: (i) smooth, bifurcate chaetae,
350 erected dorsally (Fig. 6A, Fig 7A-D), present on first four chaetigers; (ii) thick, bowed,
351 bifurcate chaetae (20-25 in number, all smooth and shorter than that of the length to
352 dorsal and accessory cirri) with distal end stout and directed toward the posterior end of
353 the body (Fig. 6B; Fig 7E-F), present up to chaetiger 4; (iii) bifurcate harpoon with
354 serrated outer edge present from fifth chaetiger onward; 30 to 35 per notopodium in mid
355 chaetigers; secondary fang is one-third the length of the main fang; deep groove between
356 both fangs; serrated zone with 24 to 27 lateral serrations (Fig. 6C; Fig. 7G-H); and (iv)

357 short, stout, unidentate chaetae with acicular shape, three to five in number and located
358 dorsally to notochaetae fascicle (Fig. 6D; Fig 7I).

359 Neurochaetae white in color, finer, longer and more abundant relative to
360 notochaetae (~11:3 in abundance). Dorsal neurochaetae longer than ventral neurochaetae.
361 Neurochaetae of three types: (i) thin, long and distally bifurcated with short distance and
362 deep groove between main fang and secondary tooth (Fig. 6E; Fig. 7J-K), around 70 to
363 90 chaetae per dorsal neuropodium; (ii) less abundant, short, stout, bidentate located
364 ventrally and positioned posterior to ventral cirrus, around 20 per neuropodium, acicular
365 chaetae not present in this bundle (Fig. 6F); and (iii) unidentate chaetae with acicular
366 shape that encircle the long, bifurcate chaetae, between seven to fifteen by neuropodium
367 (Fig. 6G; Fig 7L). Neuroaciculae abundance increments from anterior to posterior
368 segments. Ceratophore of neuropodium inserted after and down of the ventral fascicle of
369 neurochaetae (Fig. 6G). Length of neurochaetae and dorsal cirrus relatively similar.
370 Neurochaetae in the last four chaetigers short, less abundant and not exceeding the distal
371 end of the pygidial cirri (Fig. 6G).

372

373 *Taxonomic remarks.* Traditionally, *Chloeia* species have been separated by their dorsal
374 pigmentation patterns, the number of the chaetiger where branchiae start, and the relative
375 length of ventral cirri of chaetiger 2 (Horst, 1910). Recently, new features have been
376 added, such as the size proportion between anterior and posterior eyes, the type of
377 branchial ramification (pinnate vs. bipinnate), size trends of branchiae along the body,
378 and the type of chaetae present (Yáñez-Rivera & Salazar-Vallejos, 2022; Salazar-Vallejo,
379 2023). The taxonomic arrangement of the 43 currently valid species of *Chloeia* (including
380 *C. rozbaczyloi* sp. nov.) (Read & Fauchald 2023; Yáñez-Rivera & Salazar-Vallejo, 2022;
381 Salazar-Vallejo, 2023) is summarized in Table 1.

382 According to morphological characteristics, Salazar-Vallejo (2023) established
383 five groups for *Chloeia* species (Table 1) and named each after their typical species (i.e.
384 *flava*, *venusta*, *viridis*, *tumida*, and *kudenovi*). Species in the *venusta* group present
385 bippinate branchiae from chaetiger 4, progressively decreasing in size, and a single
386 middorsal band (Salazar-Vallejo, 2023). The *venusta* group currently includes *C. nuriae*
387 *C. piotrowskiae*, *C. poupini*, and *C. venusta*. According to the above-mentioned
388 characteristics, *C. rozbaczyloi* sp. nov. fits into this group.

389 Within the *venusta* group, *Chloeia rozbaczyloi* sp. nov. differs from *C. nuriae*
390 (Gulf of California to Ecuador) because the latter species has anterior eyes that are 3×

391 larger than posterior ones, a reddish middorsal, a noncontinuous longitudinal band, and a
 392 black caruncle tapered with 21 vertical folds. *Chloeia piotrowskiae* (Philippines) differs
 393 in having a regular middorsal band not constricted posteriorly, a caruncle with plicate
 394 median ridge and about 30 vertical folds (most marked by dorsal, abundant blackish
 395 spots), partially concealing lateral lobes, and bipinnate branchiae in median segments
 396 with 14–16 lateral branches, each with few secondary filaments. *Chloeia rozbaczyloi* sp.
 397 nov. differs from *C. poupini* (French Polynesia) by the latter species having a blackish
 398 anterior prostomial area; a wide middorsal band that is continuous along each segment
 399 and that is medially separated along a few anterior chaetigers; a caruncle that is darker
 400 than the adjacent body wall, that is contracted, bent laterally, reaching chaetiger 4, that is
 401 without dorsal black spots but has a median ridge with about 30 vertical folds; and median
 402 segments with branchiae with 7–8 lateral branches, each with few secondary filaments.
 403 *Chloeia venusta* (Northeastern Atlantic to Morocco and Italy) differs in having a
 404 prostomium that is anteriorly entire, pairs of minute, blackish eyes (anterior pair is slightly
 405 larger than the posterior ones), and a caruncle that is pale, slightly surpassing chaetiger 4,
 406 with a line of 12 coalescent spots and a plicate median ridge with about 25 vertical folds.

407 In *Chloeia rozbaczyloi* the caruncle reaches chaetiger 4, with a median plicate
 408 lobe with 16 to 20 vertical folds and with 10 to 14 dorsal black spots, decreasing in size
 409 to the posterior end.

410

411 The following key is proposed to identify *Chloeia* species of the *venusta* group:

412

- 413 1a. Caruncle median ridge with ≤ 20 vertical folds.....*C. rozbaczyloi* sp. nov.
 414 1b. Caruncle median ridge with ≥ 20 vertical folds.....2
 415 2a (1b) Caruncle with 21 to 25 vertical folds3
 416 2b (1b) Caruncles with > 25 vertical folds4
 417 3a (2a) Anterior eyes about 8 \times larger than posteriors*C. nuriae*
 418 3b (2a) Eyes minute, anterior eyes slightly larger than posterior ones...*C. venusta*
 419 4a (2b). Branchiae with 14–16 lateral branches.....*C. piotrowskiae*
 420 4b (2b). Branchiae with 7–8 lateral branches*C. poupini*

421

422 The known bathymetric range of *Chloeia rozbaczyloi* sp. nov. (211 to 230 m
 423 depth) is much restricted compared with other central and eastern Pacific species (e.g. *C.*
 424 *murrayae*, 30 to 200 m depth; *C. nuriae*, 13 to 210 m depth; *C. pseudeglochis*, 12 to 270

425 m depth), but is close to that of *C. pinnata* (166 to 305 m depth) and shallower than *C.*
426 *poupini* (860 m depth) (Salazar-Vallejo, 2023).

427

428 *Meristic remarks.* The total number of analyzed individuals = 64. Average length: $26.5 \pm$
429 7.2 mm (mean \pm SD); average wet weight: 0.4 ± 0.3 g; average number of segments: 30
430 ± 1.6 segments. Total weight (TW)-Length (TL) relationship was: $TW = 0.0945 e^{0.0532 TL}$;
431 $r^2 = 0.5951$) and the total length (TL) versus the number of segments (NS) was: $NS =$
432 $0.1345 TL + 26.415$; $r^2 = 0.3772$. *Chloeia rozbaczyloi* nov. sp. could be considered a
433 mid-sized species (up to 50 mm in total length). Although some shallow-waters species
434 attain a rather large size (*C. tumida*, 162 mm in length; *C. flava*, 140 mm), the trend is
435 that deep-water species tend to be smaller (> 500 m depth; < 24 mm length) (Salazar-
436 Vallejo, 2023). *Chloeia rozbaczyloi* sp. nov. differs in its larger size (26.5 ± 7.2 mm
437 length) and higher number of chaetigers (26-35) than other deep-water species *C.*
438 *kudenovi* (750 to 1,045 m; 24 mm; 24 chaetigers), *C. pocicola* (~ 750 m; 6 to 20 mm
439 length, 17 to 24 chaetigers), and *C. fiegei* (740 to 745 m; 22 mm, 28 chaetigers).
440 Additional morphometric parameters based on SEM photos of a paratype specimen
441 (SCBUCN 6982) for *C. rozbaczyloi* sp. nov. are presented in Supplementary Material
442 Table S8.

443

444 *Etymology.* The species is named after Prof. Nicolás Rozbaczyló, for his outstanding
445 dedication and notable contributions to the taxonomy and ecology of Chilean Polychaeta
446 since 1973.

447

448 *Geographic and bathymetric distribution.* Only known from the type locality (seamount
449 SFX, 25.079°S, 82.006°W, ~220 m depth) and from seamount SPG4 (25.408°S,
450 81.769°W, ~211 m depth), both within the NDMP.

451

452 *Genetic analyses*

453 A 7294 bp fragment containing the complete 18S rRNA gene, ITS1, the complete
454 5.7S rRNA gene, ITS2, and a partial 28S rRNA gene (GenBank accession OM 135245)
455 and a 16,395 bp (estimated length) partial mitochondrial genome (OM 144973) of *C.*
456 *rozbaczyloi* sp. nov. were recovered. Unrecovered regions of the mitochondrial genome
457 include (1) an estimated 34 bp of the *COX2* gene, (2) an unknown number of bases in the
458 intergenic region containing the control region (between the *COX3*-tRNA^{Lys} and

459 tRNA^{Gln}-*ND6* genes), (3) an estimated 24 bp in the *ND5* gene, and (4) an estimated 450
460 bp from the *ND4L* gene (estimated 171 bp missing) into the *ND4* gene (estimated 286 bp
461 missing) (Supplementary Material Table S7). Numerous ambiguities were present in the
462 intergenic region containing the control region that likely represents differences between
463 copies of a 730 bp repeated region (Supplementary Material Table S7). The recovered
464 mitochondrial genome consists of 13 protein-coding genes, 23 tRNA genes, and 2 rRNA
465 genes and had a nucleotide composition of 29.5% A, 22.0% C, 13.7% G, and 34.8% T
466 (excluding missing and ambiguous bases). GC content of the complete mitochondrial
467 genome (less missing bases) was 35.7%, and GC content of genes were 20.0-46.2%
468 (Supplemental material Table S7). Protein-coding genes terminated in a TAA codon or
469 an incomplete codon (T--), and, except for the *ND2* gene, amino acid sequence similarity
470 was higher than nucleotide similarity when compared to *C. pocicola* (Supplemental
471 material Table S7).

472 Bayesian and ML phylogenetic reconstruction based on the concatenated 28S
473 rRNA, 16S rRNA, and *COI* gene fragments recovered a *Chloeia* clade sister to the
474 *Notopygos* clade with moderate (> 90 PP, > 70 BP) to strong (> 95 PP, > 85 BP) support
475 for the relationships among *Chloeia* species, except for *Chloeia pocicola*, the most basal
476 species in the *Chloeia* clade (Fig. 8). *Chloeia rozbaczyloi* sp. nov. was basal to the other
477 *Chloeia* species and was most genetically similar to *C. bimaculata* (95.4%) and *C. viridis*
478 (95.2%) based on the concatenated alignment; within *Chloeia*, interspecific genetic
479 distances were 2.4-8.5% (Supplementary Material Table S2). Alignments and
480 reconstructed phylogenies based on each of the gene fragments likewise support *Chloeia*
481 *rozbaczyloi* sp. nov. being in a clade with the other *Chloeia* spp. with genetic distances
482 larger than reported for *Chloeia* spp. conspecifics and consistent with *Chloeia*
483 interspecific values (Supplementary Material Tables S3-6 and Figure S1). The
484 evolutionary relationships among Archinominae genera *Chloeia*, *Archinome*, and
485 *Notopygos* were not well supported (< 85 PP, < 50 BP). In single-gene phylogenetic
486 reconstructions (Supplementary Material Figure S1), the evolutionary relationships
487 within and among Archinominae genus clades differed.

488

489 Discussion

490 The description of *C. rozbaczyloi* sp. nov. currently increases the total number of
491 species in the genus to 43 (Read and Fauchald, 2023; Salazar-Vallejo, 2023), and of the

492 Chilean Amphinomidae species to seven, being the first formal species of the genus
493 reported for the Nazca Ridge (Rozbaczylo, 1985; Cañete, 2017). *Chloeia rozbaczyloi* sp.
494 nov. inhabits the Temperate South America biogeographic province (nr. 46 in Spalding
495 et al. [2007]) and is the first report of the family for the Juan Fernández and Desventuradas
496 Islands ecoregion (nr. 179). Future studies in this poorly explored area will reveal if the
497 new species distributes in other seamounts than the two in which it has been recorded so
498 far. However, Yáñez-Rivera and Salazar-Vallejo (2022) suggest that *Chloeia* from
499 tropical and subtropical Eastern Pacific seem to have restricted geographic distributions,
500 with notable diversification in the Indian and Indo-West Pacific Ocean.

501 *Chloeia rozbaczyloi* sp nov. seems to inhabit low-oxygen seamount ecosystems
502 of the NDMP. At ~25°S the SE Pacific Oxygen Minimum Zone (OMZ) could intrude
503 offshore to ~2,000 km westward with a vertical extension >200m depth (Palma and Silva,
504 2006, Cañete and Häussermann 2012, Dewitte et al. 2021), reaching the summits of
505 seamounts of the easternmost area of the NDMP. We speculate that lower bottom oxygen
506 conditions were present at SFX (as indicated by the presence of numerous dead
507 myctophids [Fig. 2G]) and could occur periodically in association with the seasonal
508 fluctuation of the SE Pacific OMZ and westward drift of low-oxygen mesoscale eddies,
509 which could relate to the relatively high abundance of *Chloeia rozbaczyloi* sp. nov.
510 observed. Similar oceanographic and geological conditions seem to prevail on the
511 easternmost Nazca Ridge seamounts (Palma and Silva, 2006; Fuenzalida et al., 2009;
512 Dewitte et al., 2021). From an ecological approach, amphinomids constitute a group well
513 known to thrive in benthic habitats overlaid by oxygen-deficient waters, be tolerant to
514 hypoxia and thrive in reducing settings (Barroso and Paiva, 2011; Borda et al., 2015). For
515 example, *Paramphinome australis* living at low oxygen concentrations of 0.52 ml L⁻¹, is
516 the predominant polychaete along the Chilean continental margin at 400 m depth off the
517 coast of Concepción, Chile (~36°S), comprising 42% of all polychaetes in this region
518 (Gallardo et al., 2004). Other Archinomidae, including *Chloeia* species, are reported from
519 regions with persistent OMZs, for which they may be well adapted in morphology and
520 ecological function. For example, Purchke et al. (2017) reported that in the amphinomid
521 *Eurythoe complanata*, ventilation is facilitated by longitudinal ciliary bands. Thus, the
522 ciliated accessory dorsal cirri present in some species of *Chloeia*, including *C.*
523 *rozbaczyloi* sp. nov., could likewise serve to provide enhanced ventilation where oxygen-
524 deficient conditions prevail. Wang et al. (2019) also referred to accessory dorsal cirri
525 functioning as branchial cirri. Notable abundances of *C. pinnata* are reported in offshore

526 areas off California (Jones and Thompson, 1987) where persistent OMZ occurs and
527 relatively strong currents result in the winnowing of finer detrital sediments and the
528 development of coarse sediments rich in biogenic calcium carbonate components.

529 In contrast to the low abundance and frequency of other amphinomids, such as
530 *Linopherus annulata* that live in oxygenated waters in shallow estuarine areas of the
531 Aysen fjord, southern Chile (Cañete et al., 1999), a comparatively high density of *C.*
532 *rozbaczyloi* sp. nov. was observed on the summit of seamount SFX (Figs. 2 B-F). In these
533 habitats, polychaete species could play important ecological roles (e.g., carrion-feeding)
534 as has been suggested for some amphinomid populations (mainly species of *Chloeia*)
535 associated with sand and mud (Fauchald and Jumars, 1979; Salazar-Vallejo, 2023). This
536 role may be substantially larger where amphinomids are locally abundant, such as in low-
537 oxygen environments in which *C. pinnata* inhabits, and seamount SFX where *C.*
538 *rozbaczyloi* sp. nov. is present. Potential food sources for *C. rozbaczyloi* sp. nov. include
539 foraminifera and anthozoans, which were observed in large numbers at seamount SFX
540 (Fig. 2A; Tapia-Guerra et al., 2021). Foraminifera have been reported as prey for *C.*
541 *kudenovi* (Barroso and Paiva 2011) and *C. pinnata* (Jones and Thompson, 1987).
542 Foraminifera contributed 11% to gut contents and were present in the guts of 37% of *C.*
543 *pinnata* collected off the California coast (Jones and Thompson, 1987). Other species
544 have been reported to prey on anthozoans (Fauchald and Jumars, 1979).

545 The only previous comprehensive study of the fauna of the Nazca and Salas y
546 Gomez Ridges, conducted on 22 seamounts, was by Parin et al. (1997). Of the 192 species
547 of benthic invertebrates reported in that study, 10 were polychaete taxa, among which the
548 genus *Chloeia* is mentioned, but without providing any further taxonomic or ecologic
549 details. Given the scarce knowledge of the deep-water fauna associated with seamounts
550 within this area, it is too early to discuss the endemism patterns of the species described
551 here. Nevertheless, its occurrence at only two seamounts of the seven seamounts sampled
552 (ranging from 105 to 305 m depth) in the present study preliminarily suggests it has a
553 limited distribution. Juan Fernández and the Desventuradas Islands bear among the
554 highest endemism levels in the world for coastal and shallow marine ecosystems
555 (Friedlander et al., 2016; Wagner et al., 2021). Recent reports of potential endemism in
556 this region include other benthic invertebrates, such as echinoderms (Mecho et al., 2020),
557 new species of gastropods (Sellanes et al., 2019), and polychaetes (Díaz-Díaz et al.,
558 2020), supporting the potential endemism for *Chloeia rozbaczyloi* sp. nov.

559 *Chloeia rozbaczyloi* sp. nov. is erected based on recent diagnostic taxonomic
560 features and DNA analysis. From the morphological viewpoint, *Chloeia rozbaczyloi* sp.
561 nov. can be distinguished from other species of the genus inhabiting the Pacific Ocean
562 mainly by (i) the chromatic patterns of the dorsum (middorsal dark band, or *venusta*
563 group, after Salazar-Vallejo (2023)) and the caruncle (with 16 to 20 vertical folds and
564 between 12 to 14 black spots decreasing in diameter); (ii) by the bi-annulated dorsum of
565 the first ten chaetigers, each with a bean-shaped anterior pseudosegment; (iii) long
566 neuropodial cirri, with a short ceratophore, at chaetiger 2 and reaching chaetiger 6; and
567 (iv) bipinnate branchiae from chaetiger 4, progressively decreasing in size to posterior
568 end, with seven to nine lateral branches arising from the primary, with each possessing
569 up to five pinnules. Prior studies have evaluated the phylogenetic relationship within
570 Archinominae and Amphinomidae (Borda et al., 2012, 2015; Barroso et al. 2021) based
571 on analyses of single-gene and concatenated gene datasets. Although the primary purpose
572 of our phylogenetic analyses was to provide additional evidence to confirm the
573 designation of *C. rozbaczyloi* sp. nov., the analyses were consistent with prior
574 phylogenies in the lack of congruence between single-gene trees (Wang et al., 2019) and
575 concatenated gene trees and the poor support for relationships among Amphinomidae
576 genera. This lack of support may largely be due to the few representatives of each genus
577 and family for which genetic data are available and outgroup selection (Lecointre et al.,
578 1993; Graybeal, 1998). Therefore, without greater taxonomic coverage in phylogenetic
579 reconstructions, the relationships among species and genera in phylogenetic trees may
580 not reflect the true evolutionary history. Nevertheless, the data is sufficient to support *C.*
581 *rozbaczyloi* sp. nov. being a distinct species from those with available genetic data. For
582 example, the pairwise genetic distances between *C. rozbaczyloi* sp. nov. and its congeners
583 (4.6-7.3) are comparable to or greater than those observed among the other *Chloeia*
584 congeners (2.4-8.5) based on the concatenated data set (Supplementary Material Table
585 S2). Single-gene alignments and phylogenetic reconstructions (Figure S1) further
586 support *C. rozbaczyloi* sp. nov. being a distinct species from those included in genetic
587 analyses because the genetic distances are within the range of *Chloeia* interspecific
588 genetic distances (2-20) and considerably larger than conspecific distances (<2) in
589 *Chloeia* (Tables S3-6). Thus, *C. rozbaczyloi* sp. nov. is genetically distinct from
590 congeners for which sequence data are available and it is most genetically similar to *C.*
591 *bimaculata* and *C. viridis* (Fig. 6). Only one *Chloeia* species, *C. pocicola*, has a complete
592 mitochondrial genome available for comparison to the mitochondrial genome of *C.*

593 *rozbaczyloi* sp. nov. They have the same gene order, which differs from the other
594 amphinomid mitochondrial genomes (*Eurythoe complanata* and *Cryptonome barbada*)
595 in the position of the tRNA-Lys gene (Barroso et al., 2021). The presence of a large,
596 repeated region with some differences in copies is also reported in *C. pocicola* (377 bp);
597 however, it is nearly double the length in *C. rozbaczyloi* sp. nov. (730 bp). These data
598 support that mitochondrial gene order is conserved within Amphinomidae as suggested
599 by Barroso et al. (2021). Because we were unable to recover the complete mitochondrial
600 genome, we cannot make further comparisons to amphinomid mitochondrial genomes.
601 The dataset on *Chloeia* sequences is limited, covering only six of the 43 described species
602 (Salazar-Vallejo 2023), so there remains a large potential to reconstruct the evolutionary
603 history of this taxon and to understand how local ecological and evolutionary forces
604 operate to govern the observed diversification in phenotype and genotype across different
605 realms, provinces, and ecoregions (*sensu* Spalding et al., 2007), of the tropical,
606 subtropical, and deep-sea habitats of the three oceans they occupy. Such potential is
607 currently limited by the lack of inclusion of integrative systematics for species
608 descriptions, such that species are still being described without the inclusion of some
609 genetic data for support and comparison. Thus, systematics of Amphinomidae and all
610 future descriptions should include at least some genetic data to fill this knowledge gap.

611 Seamount ecosystems are areas of high ecological relevance as they can harbor
612 endemic and rare species, and provide suitable habitats to support the populations of many
613 species of invertebrates and fishes (Friedlander et al., 2016). The present work increases
614 the current knowledge of the biodiversity associated with the seamounts of the NDMP;
615 however, further work is necessary to understand the role of this species in the ecosystem,
616 its relationship with the OMZ, and to elucidate biogeographic connections within and
617 among seamount ecosystems in this ecoregion as well as in others of the Southeastern
618 Pacific Ocean.

619 **Acknowledgments:** The authors wish to thank the crew of the *AGS 61 Cabo de Hornos*
620 for the facilities granted during the CIMAR 22 “Oceanic Islands” cruise. Special thanks
621 also go to OCEANA for the support provided in the field with the ROV operation, and to
622 María Valladares and EPIC cruise participants for field assistance. Jan M. Tapia-Guerra
623 and Jorge Avilés (SCBUCN) are also acknowledged for help with Figure 2. Marco León
624 helped with the design of Figures 5 and 7. Permit for sampling during the CIMAR 22
625 cruise was granted by Sub-secretaría de Pesca y Acuicultura, Chile, Resolution N° 3314.

626 The comments and suggestions of three anonymous reviewers greatly helped to improve
627 the manuscript.

628 **Funding:** This study was funded by: Comité Oceanográfico Nacional de Chile (CONA)
629 grant C2216-09 to JS. ANID- Millennium Science Initiative ESMOI and ANID-ATE
630 22004 BioDUCCT, FONDEQUIP EQM150109, and FONDECYT 1181153 to JS and
631 AM. Elaboration of the manuscript was partially supported by CONA-UMAG, Grant
632 UMAG060807 CIMAR 26 Oceanic Island to JIC, OCEANA Chile provided the ROV
633 and pilot.

634

635 **Conflict of interest:** The authors declare that they have no conflict of interest.

636

637 **Ethical approval:** All applicable international, national, and/or institutional guidelines
638 for the care and use of animals were followed by the authors.

639

640 **Sampling and field studies:** All necessary permits for sampling and observational field
641 studies have been obtained by the authors from the competent authorities and are
642 mentioned in the acknowledgments.

643

644 **References**

645 Barroso R, Paiva PC (2011) A new deep-sea species of *Chloeia* (Polychaeta:
646 Amphinomidae) from southern Brazil. J Mar Biol Ass UK 91(2): 419–423

647 Barroso R, Kudenov JD, Shimabukuro M, Carrerette O, Sumida PYG, Paiva PC, Seixas
648 VC (2021) Morphological, molecular and phylogenetic characterization of a new
649 *Chloeia* (Annelida: Amphinomidae) from a pockmark field. Deep-Sea Research
650 Part I, 171(17):103499. DOI: 10.1016/j.dsr.2021.103499.

651 Bernt M, Donath A, Jühling F, Externbrink F, Florentz C, Fritzsche G, Pütz J, et al. (2013).
652 MITOS: Improved de novo metazoan mitochondrial genome annotation. Mol
653 Phylogenet Evol 69:313–19

654 Böggemann M (2009). Polychaetes (Annelida) of the abyssal SE Atlantic. Organisms
655 Diversity and Evolution 9 (4): 251-428

656 Borda E, Kudenov JD, Bienhold C, Rouse GW (2012) Towards a revised Amphinomidae
657 (Annelida, Amphinomida): description and affinities of a new genus and species
658 from the Nile Deep-sea Fan, Mediterranean Sea. Zool Scr 41(3): 307-325

- 659 Borda EB, Yáñez-Rivera B, Ochoa GM, Kudenov JD, Sánchez-Ortiz C, Schulze A,
660 Rouse GW (2015) Revamping Amphinomidae (Annelida: Amphinomida), with
661 the inclusion of *Notopygos*. Zool Scr 44: 324-333
- 662 Cañete, J.I. and V. Häussermann (2012) Colonial life under Humboldt Current system:
663 deep sea coral from O'Higgins I seamount. Lat Am J Aquat Res 40: 467-472
- 664 Cañete JI (2017) New record of *Pherecardia striata* (Polychaeta: Amphinomidae) from
665 Easter Island, Chile. Lat Am J Aquat Res 45: 199-202
- 666 Cañete JI, Leighton GL, Aguilera FF (1999) Polychaetes from Aysén Fjord, Chile:
667 distribution, abundance and biogeographical comparison with the shallow soft-
668 bottom polychaete fauna from Antarctica and the Magellan Province. Sci Mar
669 63(1): 243-252
- 670 Dean HK (2009) Polychaetes and Echiurans. IN: Wehrtmann LS, Cortés J (eds) Marine
671 diversity of Costa Rica, Central America. Springer, Dordrecht, pp 181 – 191
- 672 Dean HK, Sibaja-Cordero JA, Cortés J (2012) Polychaetes (Annelida: Polychaeta) of
673 Cocos Island National Park, Pacific Costa Rica. Pac Sci 66: 347-386
- 674 Dewitte B, Conejero C, Ramos M, Bravo L, Garçon V, Parada C, Sellanes J, Mecho A,
675 Muñoz P, Gaymer CF (2021) Understanding the impact of climate change on
676 the oceanic circulation in the Chilean island ecoregions. Aquatic Conservation
677 Marine and Freshwater Ecosystems 31 (2): 232-252. DOI: 10.1002/aqc.3506.
- 678 Díaz-Díaz OF, Rozbaczylo N, Sellanes J, Tapia-Guerra JM (2020). A new species of
679 *Eunice* Cuvier, 1817 (Polychaeta: Eunicidae) from the slope of the
680 Desventuradas Islands and seamounts of the Nazca Ridge, southeastern Pacific
681 Ocean. Zootaxa 4860 (2): 211-226 DOI: 10.11646/zootaxa.4860.2.4
- 682 Easton EE, Hicks D (2020) Complete mitogenome of *Carijoa riisei* (Octocorallia:
683 Alcyonacea: Stolonifera: Clavulariidae). Mitochondrial DNA Part. B. 5,
684 1826–1827. <https://doi.org/10.1080/23802359.2020.1750998>
- 685 Fauchald K (1977) Polychaetes from intertidal areas in Panama with a review of previous
686 shallow-water records. Sm C Zool 221:1-81
- 687 Fauchald K, Jumars PA (1979) The diet of worms: a study of polychaete feeding guilds.
688 Oceanogr Mar Biol 17: 193-284
- 689 Felsenstein J (1981) Evolutionary trees from DNA sequences: a maximum likelihood
690 approach. J Mol Evol. 17(6): 368-376. doi: 10.1007/BF01734359
- 691 Friedlander AM, Ballesteros E, Caselle JE, Gaymer CF, Palma AT, Petit I, Varas E,
692 Muñoz W, Sala E (2016) Marine Biodiversity in Juan Fernández and

- 693 Desventuradas Islands, Chile: Global Endemism Hotspots. PloS one [https://](https://doi:10.1371/journal.Pone.0145059)
694 doi:10.1371/journal.Pone.0145059
- 695 Fuenzalida R, Schneider W, Garcés-Vargas J, Bravo L, Lange C (2009) Vertical and
696 horizontal extension of the oxygen minimum zone in the eastern South Pacific
697 Ocean. Deep-Sea Res Pt II 56: 992–1003
- 698 Gallardo VA, Palma M, Carrasco FD, Gutiérrez D, Levin LA, Cañete JI (2004)
699 Macrobenthic zonation caused by the oxygen minimum zone on the shelf and
700 slope off Central Chile. Deep-Sea Res Pt II 51: 2475–2490
- 701 Gálvez-Larach M (2009) Montes submarinos de Nazca y Salas y Gómez: una revisión
702 para el manejo y conservación. IN: Arana P, Pérez JAA, Pezzuto PR (eds) Deep-
703 sea fisheries of Latin America. Lat Am J Aquat Sci 37: 479-500
- 704 Graybeal A (1998) Is It Better to Add Taxa or Characters to a Difficult Phylogenetic
705 Problem? Systematic Biology 47(1): 9-17.
- 706 Hartman O (1959) Catalogue of the polychaetous annelids of the world. Part I and II. Occ
707 Pap Allan Hancock Found 23: 1-628
- 708 Horst R (1912) Polychaeta errantia of the Siboga Expedition. Brill EJ (ed) 24a: 1-43
- 709 Huelsenbeck JP, Ronquist F (2001) MRBAYES: Bayesian inference of phylogenetic
710 trees. Bioinformatics, 17, 754-755. doi:10.1093/bioinformatics/17.8.754
- 711 Jones GF, Thompson BE (1987) The distribution and abundance of *Chloeia pinnata*
712 Moore, 1911 (Polychaeta: Amphinomidae) on the Southern California
713 borderland. Pac Sci 41: 122-131
- 714 Kohn A, Lloyd MC (1973) Marine polychaetes annelids of Eastern Island. Int Rev
715 Hydrobiol 58: 691-712
- 716 Kudenov J (1991) A new family and genus of the order Amphinomida (Polychaeta) from
717 Galapagos hydrothermal vents. Ophelia 5: 111–120
- 718 Kudenov J (1993) Amphinomidae and Euphrosinidae (Annelida: Polychaeta) principally
719 from Antarctica, the Southern Ocean and Subantarctic region. Antar Res Ser 58:
720 93-154
- 721 Kudenov J (1995) Family Amphinomidae Lamarck, 1818. Taxonomic Atlas of the
722 Benthic Fauna of the Santa Maria Basin and Western Santa Barbara Channel 5:
723 207–215
- 724 Lamarck JB (1818) Histoire naturelle des animaux sans vertèbres 5 : 1-612

- 725 Lanfear R, Calcott B, Ho SY, Guindon S (2012) Partitionfinder: combined selection of
726 partitioning schemes and substitution models for phylogenetic analyses. *Mol*
727 *Biol Evol.* 2012 Jun;29(6):1695-701. doi: 10.1093/molbev/mss020
- 728 Lanfear R, Frandsen PB, Wright AM, Senfeld T, Calcott B (2017) PartitionFinder 2: New
729 Methods for Selecting Partitioned Models of Evolution for Molecular and
730 Morphological Phylogenetic Analyses. *Mol Biol Evol.* 2017 Mar 1;34(3):772-
731 773. doi: 10.1093/molbev/msw260.
- 732 Lecointre G, Hervé G, Hoc Lanh Van L, Le Guyader H (1993) Species sampling has a
733 major impact on phylogenetic inference. *Molecular Phylogenetics and Evolution*
734 2 (3) : 205-224
- 735 Liñero-Arana I, Díaz O (2010) Amphinomidae and Euphrosinidae (Annelida: Polychaeta)
736 from northeastern coast of Venezuela. *Lat Am J Aquat Res* 38: 107–120
- 737 McIntosh WC (1885) Report of the Annelida Polychaeta collected by H. M. S. Challenger
738 during the years 1873-76. *Challenger Rep* 12: 1-554
- 739 Orrhage L (1990) On the microanatomy of the supraoesophageal ganglion of some
740 amphinomids (Polychaeta Errantia), with further discussion of the innervation
741 and homologues of the polychaete palps. *Acta Zool-Stockholm* 71: 45–59
- 742 Palma S, Silva N (2006) Epipelagic siphonophore assemblages associated with water
743 masses along a transect between Chile and Easter Island (eastern South Pacific
744 Ocean). *J Plankton Res* 28: 1143-1151.
- 745 Parin N, Mironov AN, Nesis KN (1997) Biology of the Nazca and Sala y Gomez
746 Submarine Ridges, an Outpost of the Indo- West Pacific Fauna in the Eastern
747 Pacific Ocean: Composition and Distribution of the Fauna, its Communities and
748 History. *Advances in Marine Biology* 32: 145-242.
749 [https://doi.org/http://dx.doi.org/10.1016/S0065-2881\(08\)60017-6](https://doi.org/http://dx.doi.org/10.1016/S0065-2881(08)60017-6)
- 750 Purschke, G., Hugenschutt, M., Ohlmeyer, L., Meyer, H. and Weihrauch, D. (2017).
751 Structural analysis of the branchiae and dorsal cirri in *Eurythoe complanata*
752 (Annelida, Amphinomida). *Zoomorphology* 136:1–18.
- 753 Read G, Fauchald, K. (Ed.) (2022). World Polychaeta Database. *Chloeia* Lamarck, 1818.
754 Accessed through: World Register of Marine Species at:
755 <https://www.marinespecies.org/aphia.php?p=taxdetails&id=129184> on 2022-
756 11-30
- 757 Rouse GW, Pleijel F (2001) Polychaetes. Oxford, University Press

- 758 Rozbaczylo N (1985) Los anélidos poliquetos de Chile. Índice sinonímico y distribución
759 geográfica de especies. Monografías Biológicas, Pontificia Universidad Católica
760 de Chile 3: 1-284
- 761 Salazar-Vallejo. S.I. (2023). Revision of *Chloeia* Savigny in Lamarck, 1818 (Annelida,
762 Amphinomidae). Zootaxa 5238: 1-134.
- 763 Salazar-Vallejo, S.I. and J.M. Orensanz. (1991). Pilárgidos (Annelida: Polychaeta) de
764 Uruguay y Argentina. Cahiers de Biologie Marine 32: 267-279.
- 765 Salazar-Vallejo SI, Carrera-Parra LF, Muir AI, León-González J, Piotrowski C, Sato M
766 (2014) Polychaete species (Annelida) described from the Philippine and China
767 Seas. Zootaxa 3842: 1-68
- 768 Sellanes J, Salisbury RA, Tapia JM, Asorey CM (2019) A new species of *Atrimitra* Dall,
769 1918 (Gastropoda: Mitridae) from seamounts of the recently created Nazca-
770 Desventuradas Marine Park, Chile. PeerJ 7:e8279 DOI 10.7717/peerj.8279
- 771 Spalding MD, Fox HE, Allen GR, Davidson N, Ferdaña ZA, Finlayson M, Halpern BS,
772 Jorge MA, Lombana A, Lourie SA, Martin KD, McManus E, Molnar JR,
773 Recchia CA, Robertson J (2007) Marine Ecoregions of the World: A
774 Bioregionalization of Coastal and Shelf Areas. BioScience 57: 573-583
- 775 Stamatakis A (2014) RAxML version 8: a tool for phylogenetic analysis and post-analysis
776 of large phylogenies. Bioinformatics, 30(9):1312–1313.
- 777 Tapia-Guerra JM, Mecho A, Easton EE, Gallardo MA, Gorny M, Sellanes J (2021) First
778 description of deep benthic habitats and communities of oceanic islands and
779 seamounts of the Nazca Desventuradas Marine Park, Chile. Scientific Reports
780 11: 6209. DOI:10.1038/s41598-021-85516-8
- 781 Wang, Z, Zhang Y, Xie YJ, Qiu J-W (2019) Two species of fire worms (Annelida:
782 Amphinomidae: *Chloeia*) from Hong Kong. Zoological Studies 58, doi:
783 10.6620/ZS.2019.58-22
- 784 Wagner D, van der Meer L, Gorny M, Sellanes J, Gaymer C, Soto EH, Easton EE,
785 Friedlander AM, Lindsay DJ, Molodtsova TN, Boteler B, Durussel C, Gjerde
786 KM, Currie D, Gianni M, Brooks CM, Shiple MJ, Wilhelm TA, Quesada M,
787 Thomas T, Dunstan PK, Clark NA, Villanueva LA, Pyle RL, Clark MR,
788 Georgian SE, Morgan LE (2021) The Salas y Gómez and Nazca ridges: A review
789 of the importance, opportunities and challenges for protecting a global diversity
790 hotspot on the high seas. Marine Policy 126: 194377. DOI:
791 doi.org/10.1016/j.marpol.2020.104377

- 792 Wiklund H, Nygren A, Pleijel F, Sundberg P (2008) The phylogenetic relationships
793 between Amphinomidae, Archinomidae and Euphrosinidae (Amphinomida:
794 Aciculata: Polychaeta), inferred from molecular data. *J Mar Biol Ass UK* 88:
795 509–513
- 796 Wilhelm TA, Sheppard CRC, Sheppard ALS, Gaymer CF, Parks J, Wagner D, Lewis NA
797 (2014) Large marine protected areas – advantages and challenges of going big.
798 *Aquat Conserv* 24 (2): 24–30
- 799 Xia X (2018) DAMBE7: New and Improved Tools for Data Analysis in Molecular
800 Biology and Evolution. *Mol Biol Evol* 35 (6): 1550-1552. doi:
801 10.1093/molbev/msy073.
- 802 Xia X, Lemey P (2009). Assessing substitution saturation with DAMBE. In P. Lemey,
803 M. Salemi, and A. Vandamme (Eds.), *The Phylogenetic Handbook: A Practical*
804 *Approach to Phylogenetic Analysis and Hypothesis Testing* (pp. 615-630).
805 Cambridge: Cambridge University Press. doi:10.1017/CBO9780511819049.022
- 806 Xia X, Xie Z, Salemi M, Chen L, Wang Y (2003) An index of substitution saturation and
807 its application *Mol. Phylogenet. Evol.*, 26 (2003), pp. 1-7
- 808 Yáñez-Rivera B, Carrera-Parra LF (2012) Reestablishment of *Notopygos megalops*
809 McIntosh, description of *N. caribea* n. sp. from the Greater Caribbean and
810 barcoding of “amphiamerican” *Notopygos* species (Annelida, Amphinomidae).
811 *Zookeys* 223: 69-84
- 812 Yáñez-Rivera B, Salazar-Vallejo SI (2022) Revision of *Chloeia* Savigny in Lamarck,
813 1818 from tropical American seas (Annelida, Amphinomidae). *Zootaxa* 5128:
814 503-537.
- 815 Yáñez E, Silva C, Vega R, Espíndola F, Álvarez L, Silva N, Palma S, Salinas S, Menschel
816 E, Häussermann V, Soto D, Ramírez N (2009) Seamounts in the southeastern
817 Pacific Ocean and biodiversity on Juan Fernández seamounts, Chile. *Lat Am J*
818 *Aquat Res* 37: 555-57
- 819

820 **Figure Captions**

821 **Fig. 1** Study area and sampling points at the Nazca Ridge and Juan Fernández archipelago
822 during CIMAR 22 and EPIC cruises. **A** Star indicates the location of seamount SFX, the
823 seamount in which the species *Chloeia rozbaczyloi* sp. nov. has been reported of all the
824 seamounts sampled during CIMAR 22 (violet dots), and the triangle indicates SPG4, the
825 seamount in which additional material of the new species was collected during the EPIC
826 cruise. **B** Blue dot indicates the initial position of the ROV transect and red dots the initial
827 and final position of the trawl transect at seamount SFX.

828

829 **Fig. 2** Frames extracted from the ROV videos obtained at the seamount SFX with *in situ*
830 observations of *Chloeia rozbaczyloi* sp. nov. **A** Representative image of the habitat,
831 dominated by calcareous coarse sediment and rhodoliths, dark spots are small anemones;
832 **B** *Chloeia rozbaczyloi* sp. nov. on the substrate near an anemone; **C**, **D** close-ups of
833 *Chloeia rozbaczyloi* sp. nov. showing live coloration; **E** an individual next to the
834 gastropod *Chryseofusus kazdailisi*; **F** individuals near the irregular echinoid
835 *Scrippsechinus fisheri*; **G** a dead fish, probably a myctophid, close to two *Chloeia*
836 *rozbaczyloi* sp. nov. individuals. Distance between the red dots of the laser pointers in **A**
837 and **B** is 10 cm.

838

839 **Fig. 3** *Chloeia rozbaczyloi* sp. nov. **A**, **B** Holotype MNHNCL-ANN-15017, **C**, **E**, **F**
840 Paratype SCBUCN-6859, **D** Paratype SCBUCN-7262. **A** whole body dorsal view, and
841 **B** ventral view; **C** dorsal view showing details of the anterior end and the black-spotted
842 pattern of the caruncle; **D** dorsal view of the anterior end showing the difference in the
843 size of the eyes and black-spotted pattern of the caruncle. Note the darker caruncle in this
844 specimen (e = eyes of left side; ca = caruncle; asterisk = anterior lobe of palp). Antennae
845 were removed to show the eyes; **E** dorsal view of chaetigers VIII and IX showing the
846 bean-shaped anterior pseudosegment (black arrows); **F** dorsum of mid chaetigers showing
847 middorsal band, screw-shaped, in a living specimen.

848

849 **Fig. 4** SEM images of *Chloeia rozbaczyloi* sp. nov. **A** Paratype SCBUCN-6982, **B**
850 paratype SCBUCN-6983, **C**, **D**, **F** paratype SCBUCN-6981, **E**, **G** paratype SCBUCN-
851 6984. **A** dorsal view of the anterior end (ca = caruncle; dc = dorsal cirrus; fbr = first pair
852 of branchiae; vc = ventral cirri; I-IV = chaetigers); detail of caruncle is shown in the left

853 corner, posterior view to shown the free zone and plicated margin; **B** dorsal view of
 854 anterior end of prostomium (plo = anterior lobe of palps; IAn = lateral antennae; MAn =
 855 Median antennae PAn = Palps antennae; **C** ventral view of anterior end (pa = palps; lg =
 856 longitudinal groove; m = mouth; vc2 and vc6 = ventral cirri 2 and 6; I-VII = chaetigers);
 857 **D** dorsal view of chaetiger 3 (ac = accessory cirri; dc = dorsal cirri); **E** detail of accessory
 858 cirri of chaetiger 3 (white arrows show lateral ciliated margin); **F** dorsal view of
 859 branchiate segments (br = branchiae; dc = dorsal cirri; na = notopodial aciculae; nl =
 860 notopodial lobe); **G** ventral view of the pygidium showing the aspect of pygidial cirri and
 861 its proportion in relation to the last chaetiger and ventral cirrus (pc = pygidial cirri; vc =
 862 ventral cirri; cp = ceratophore; cs = ceratostyle; XXIV to XXVIII = five posterior
 863 chaetigers).

864

865 **Fig. 5** *Chloeia rozbaczyloi* sp. nov. **A**, Drawing of the anterior end, dorsal view of the
 866 prostomium and the caruncle, which is presented in a laterodorsal position to show the
 867 number of vertical folds; **B** Lateral and frontal view of bipinnate branchiae of mid
 868 chaetigers.

869

870 **Fig. 6** SEM images of *Chloeia rozbaczyloi* sp. nov. notochaetae. **A** Smooth, bifurcate
 871 chaetae, erected dorsally; **B** bowed, bifurcated notochaetae of anterior parapodia,
 872 showing an insert of the distal end of this chaetae (dc= dorsal cirrus); **C** bifurcate harpoon
 873 notochaetae with serrated edge of medium and posterior parapodium; **D** notoaciculae of
 874 third chaetiger (noa= notoaciculae, ac = accessory cirri). Neurochaetae: **E** distal end of
 875 thin, bifurcated neurochaetae of mid chaetigers in two positions to show the proportion
 876 between main fang and secondary tooth; **F** bundle of posterior neurochaetae and disposal
 877 of neuroaciculae (nea); **G** anterior view of posterior parapodium showing differences in
 878 abundance and length between dorsal and ventral neurochaetae (br = branchiae, no =
 879 notopodium, ne= neuropodium).

880

881 **Fig. 7** *Chloeia rozbaczyloi* sp. nov chaetae types: **a-d** smooth, anterior bifurcate chaetae;
 882 **e-f** bowed, bifurcated notochaetae of anterior parapodia; **g-h** bifurcate harpoon
 883 notochaetae with serrated edge in two position; **i** notoaciculae of anterior chaetiger; **j-k**
 884 distal end of thin, bifurcated neurochaetae of mid chaetigers in two positions to show the
 885 proportion between main fang and secondary tooth; **l** neuroaciculae of mid chaetiger.

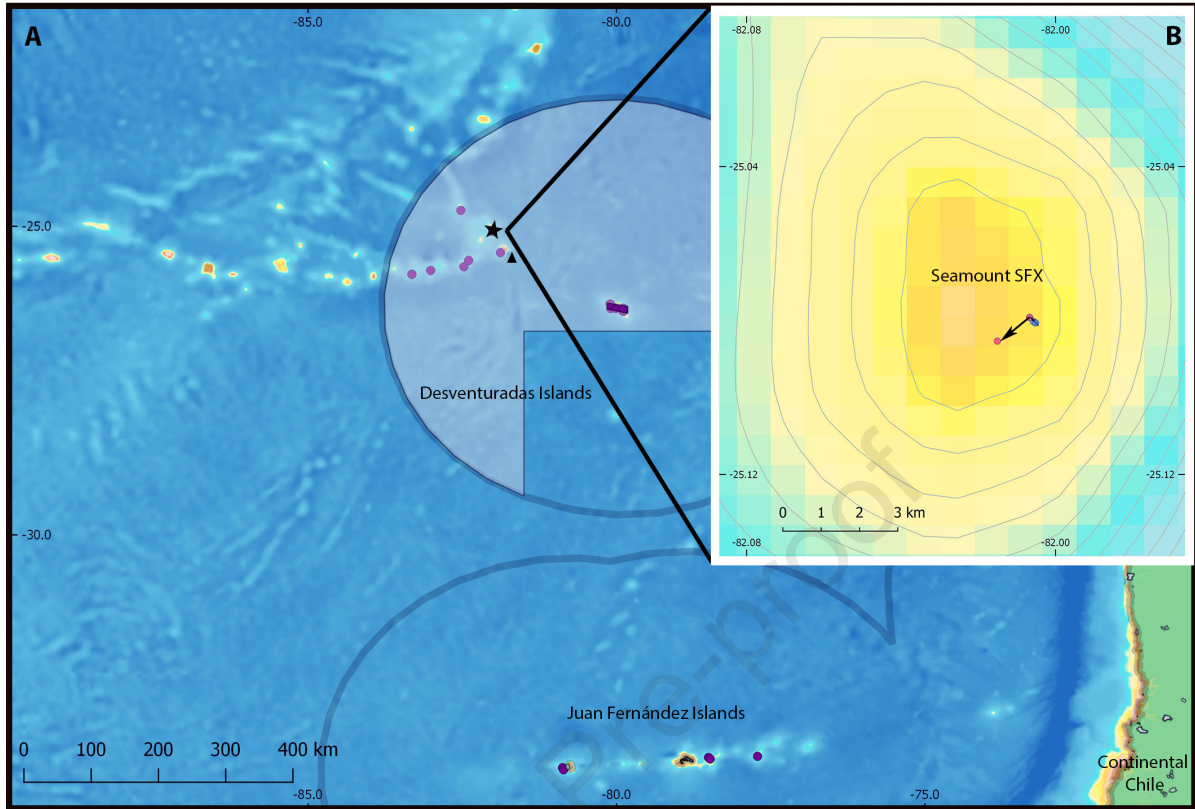
886

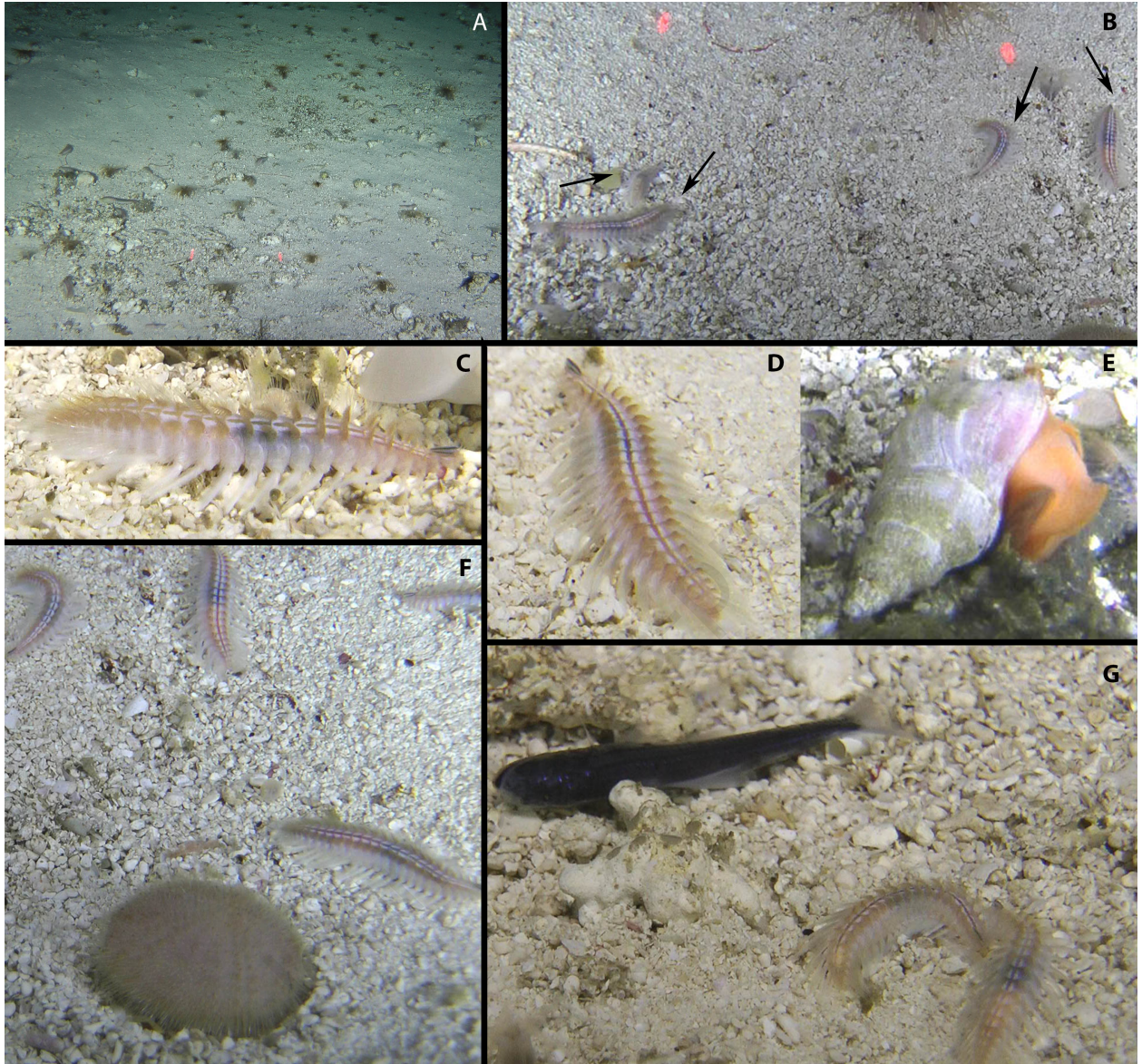
887 **Fig. 8** Bayesian phylogenetic reconstruction (50% majority consensus) of Archinominae
888 species with outgroup *Paramphinome jeffreysi* (Amphinominae) based on the 1492 bp
889 alignment of 28S rRNA + 16S rRNA + COI codon position 1 and 2 gene fragments (735
890 + 323 + 394 bp, respectively) that provides support that *C. rozbaczyloi* sp. nov. is a
891 distinct species from other *Chloeia* species for which these genetic markers are available.
892 Support values are at the nodes with "--" indicating support of < 50 BP or a node not
893 recovered in the maximum-likelihood analysis. Accession numbers and details of the
894 specimens selected are available in Table S1. Commands for phylogenetic
895 reconstructions are available in the "Scripts, job settings, and commands" section of the
896 Supplementary Material.
897

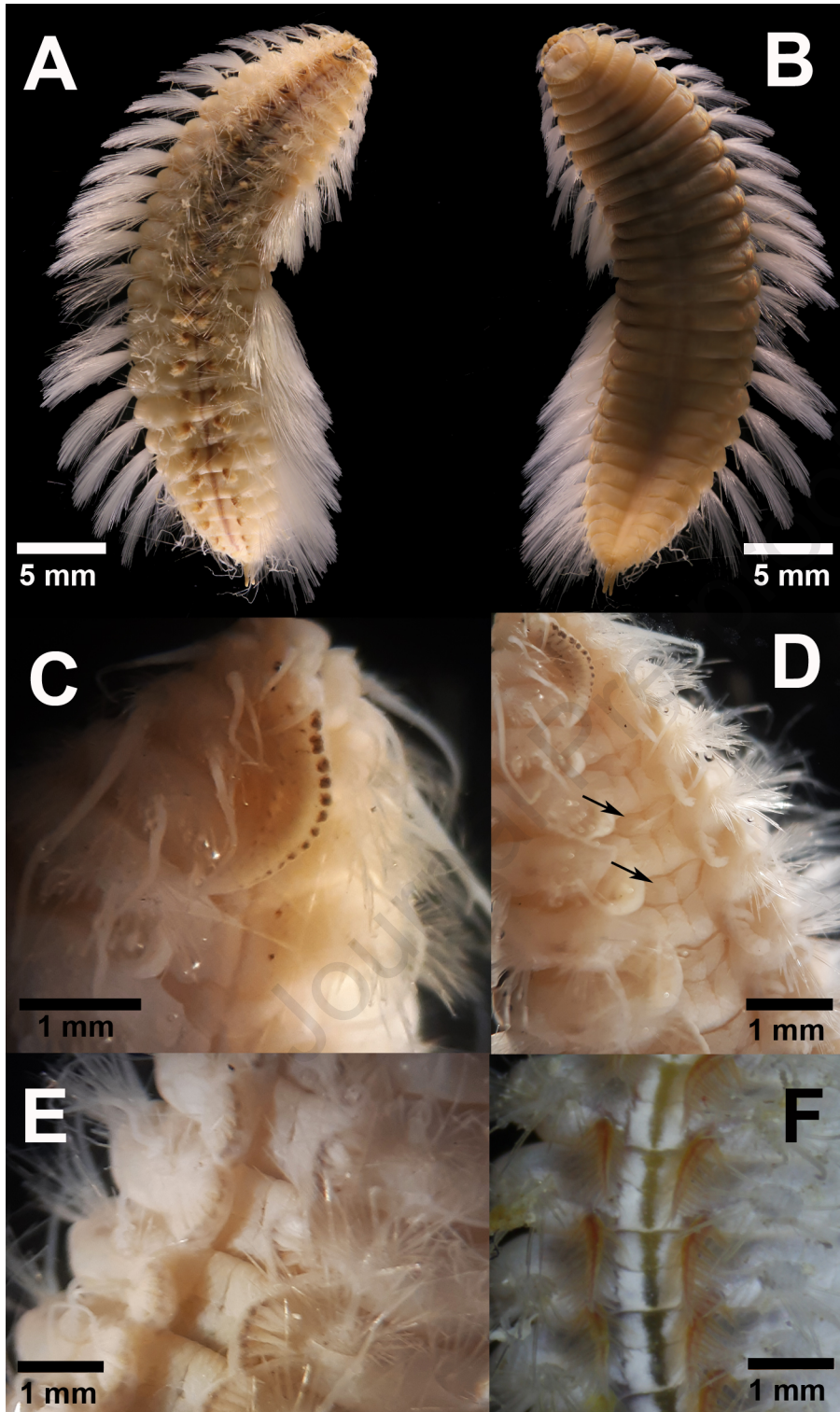
Table 1.- Main taxonomic features of *Chloeia* Savigny in Lamarck, 1818 (Polychaeta: Amphinomidae: Archinominae): type of branchiae (pinnate vs. bipinnate), chaetiger number (3, 4 or 5) in which branchiae start, and the dorsal pigmentation pattern (single middorsal bands, single middorsal spots, double longitudinal bands, complex patterns, or none). Numbers indicated in parenthesis for each *Chloeia* group, according to Salazar-Vallejo (2023), correspond to the number of species in each group. Modified from Salazar-Vallejo, 2023. The species described here is bolded. References: Yáñez-Rivera & Salazar-Vallejo (2022), Salazar-Vallejo (2023), and present study.

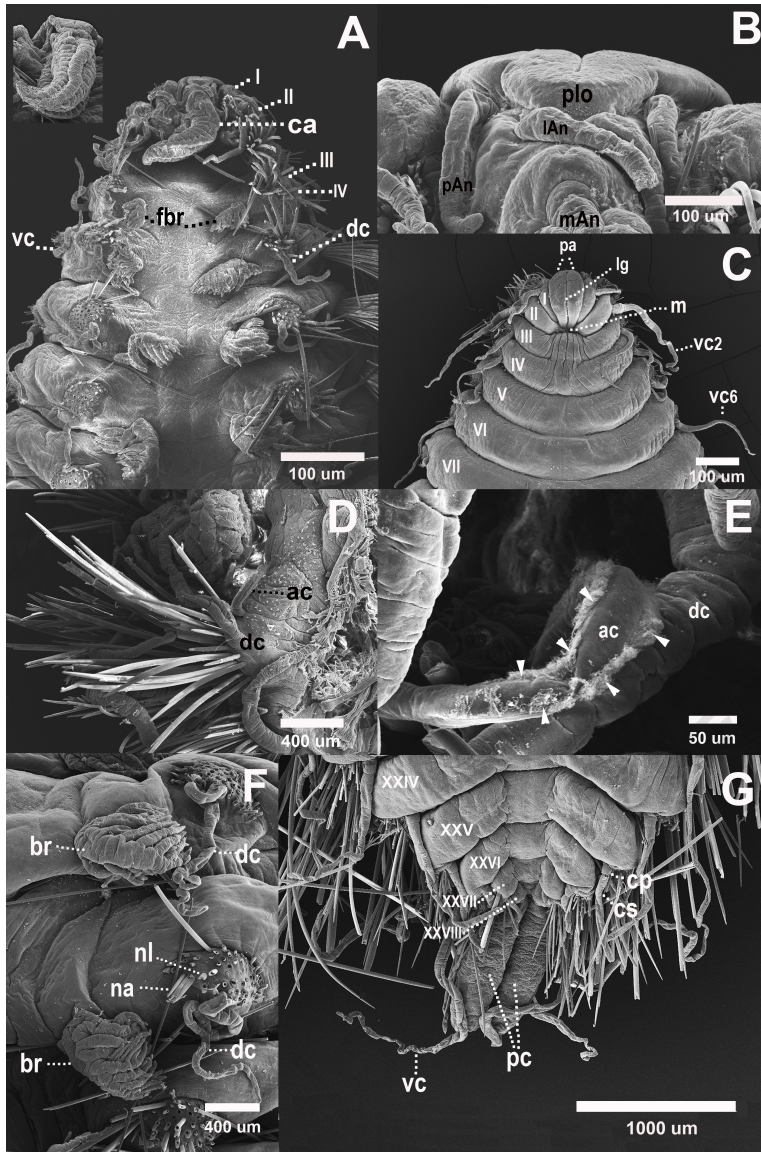
Main branchiae taxonomic feature	Chaetiger number in which branchiae start	Branchiae size characteristics	<i>Chloeia</i> group	Dorsal band characteristics	<i>Chloeia</i> species
Branchiae pinnate			<i>rosea</i> (1)		<i>C. rosea</i> Potts 1909
Branchiae bipinnate	3		<i>fucata</i> (1)		<i>C. fucata</i> de Quatrefages 1866
	4	Branchiae progressively smaller posteriorly	<i>flava</i> (3)	Middorsal spots	<i>C. flava</i> (Pallas 1766) <i>C. maculata</i> Potts 1909 <i>C. pulchella</i> Baird 1868
			<i>venusta</i> (5)	Middorsal band	<i>C. nuriae</i> Yáñez-Rivera & Salazar-Vallejo 2022 <i>C. piotrowskiae</i> Salazar-Vallejos 2023 <i>C. poupini</i> Salazar-Vallejo 2023 <i>C. rozbaczyloi</i> Cañete & Sellanes 2023 <i>C. venusta</i> de Quatrefages 1866
			<i>viridis</i> (12)	Dorsum with complex patterns of pigmentation	<i>C. amoureuxi</i> Salazar-Vallejo 2023 <i>C. amphora</i> Horst 1910 <i>C. conspicua</i> Horst 1910 <i>C. euglochis</i> Ehlers 1887 <i>C. gilleti</i> Salazar-Vallejo 2023 <i>C. hutchingsae</i> Salazar-Vallejo 2023 <i>C. incerta</i> de Quatrefages 1866 <i>C. meziane</i> Salazar-Vallejo 2023 <i>C. pseudeuglochis</i> Augener 1922 <i>C. violacea</i> Horst 1910 <i>C. viridis</i> Schmarda 1861 <i>C. zibrowii</i> Salazar-Vallejo 2023
			<i>tumida</i> (13)	Dorsum without pigmentation pattern	<i>C. bemisae</i> Salazar-Vallejo 2023 <i>C. boucheti</i> Salazar-Vallejo 2023 <i>C. entypa</i> Chamberlin 1919 <i>C. fauveli</i> Salazar-Vallejo 2023 <i>C. fiegei</i> Salazar-Vallejo 2023 <i>C. gesae</i> Salazar-Vallejo 2023 <i>C. gilchristi</i> McIntosh 1924 <i>C. keablei</i> Salazar-Vallejo 2023 <i>C. murrayae</i> Salazar-Vallejo 2023 <i>C. paulayai</i> Yáñez-Rivera & Salazar-Vallejo 2022 <i>C. pinnata</i> Moore 1911 <i>C. richeri</i> Salazar-Vallejo, 2023

					<i>C. tumida</i> Baird, 1868
		Branchiae abruptly smaller after a few chaetigers	<i>kudenovi</i> (2)		<i>C. kudenovi</i> Barroso & Paiva 2011 <i>C. pocicola</i> Barroso & Kudenov (Barroso et al. 2021)
	5		<i>fusca</i> (2)	Double middorsal bands	<i>C. bistrinata</i> Grube 1868 <i>C. fusca</i> (McIntosh 1885)
			<i>longisetosa</i> (4)	Dorsum without pigmentation pattern	<i>C. inermis</i> de Quatrefages 1866 <i>C. longisetosa</i> Potts 1909 <i>C. slapcinskyi</i> Salazar-Vallejo 2023 <i>C. wangi</i> Salazar-Vallejo 2023

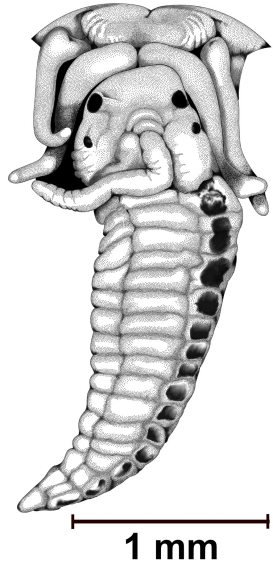




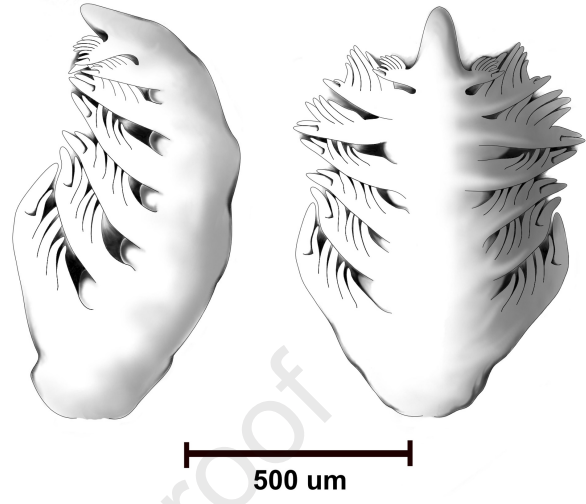




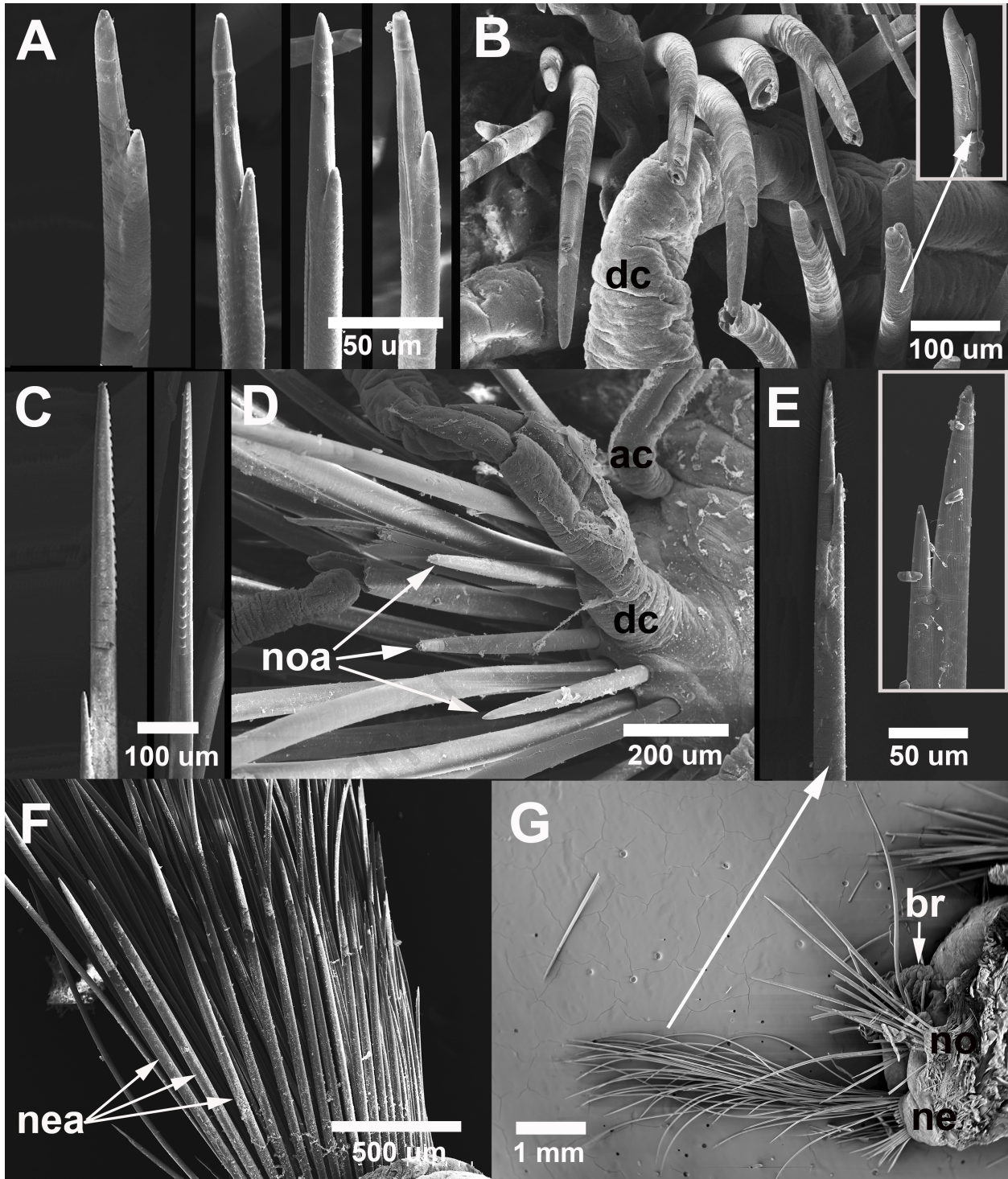
A

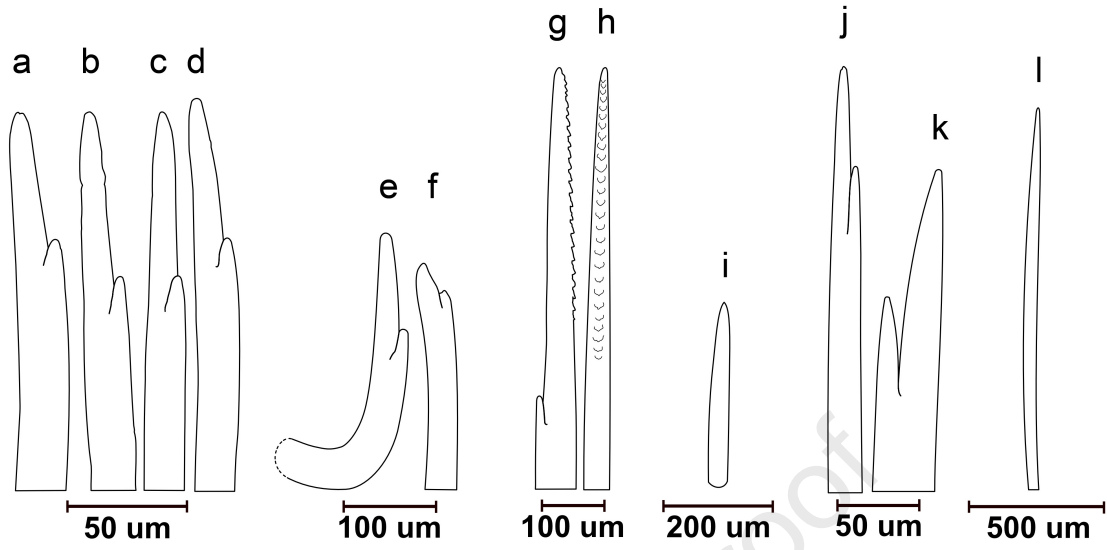


B



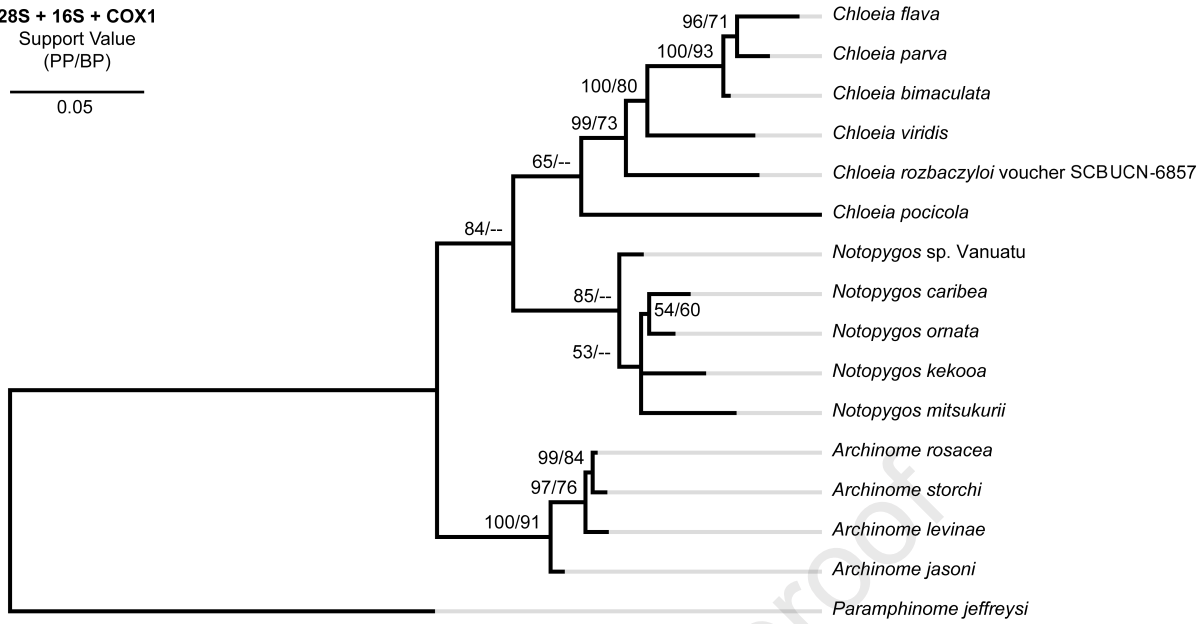
Journal Pre-proof





28S + 16S + COX1
 Support Value
 (PP/BP)

 0.05



Journal Pre-proof

- A new species of amphinomid polychaete, *Chloeia rozbaczyloi* sp. nov. is described
- The new species inhabits poorly explored seamounts of the remote Nazca Ridge off Chile
- This finding constitutes the first report of the genus *Chloeia* for Chilean waters
- Genetic data for the new species *Chloeia rozbaczyloi* sp. nov is provided
- Seamounts on which *Chloeia rozbaczyloi* sp. nov. is reported are located within the recently created Nazca Desventuradas Marine Park

Journal Pre-proof

Declaration of interests

The authors declare that they have no known competing financial interests or personal relationships that could have appeared to influence the work reported in this paper.

The authors declare the following financial interests/personal relationships which may be considered as potential competing interests:

Javier Sellanes, Ivan Canete reports financial support was provided by Comité Oceanográfico Nacional. Javier Sellanes, Erin E. Easton, Ariadna Mecho reports financial support was provided by Millenium Science Initiative ANID. Javier Sellanes reports financial support was provided by FONDEQUIP. Javier Sellanes, Ariadna Mecho reports financial support was provided by FONDECYT. Javier Sellanes reports equipment, drugs, or supplies was provided by OCEANA Chile.